ARL-TR-8006 ● Apr 2017

US Army Research Laboratory

Quasi-Static and Dynamic Characterization of Equal Channel Angular Extrusion (ECAE) – Processed and Rolled AZ31 Magnesium Alloy Sheet

by Laszlo J Kecskes, Vincent H Hammond, Michael Eichhorst, Lothar Meyer, and Norman Herzig

NOTICES

Disclaimers

The findings in this report are not to be construed as an official Department of the Army position unless so designated by other authorized documents.

Citation of manufacturer's or trade names does not constitute an official endorsement or approval of the use thereof.

Destroy this report when it is no longer needed. Do not return it to the originator.

ARL-TR-8006 ● Apr 2017

US Army Research Laboratory

Quasi-Static and Dynamic Characterization of Equal Channel Angular Extrusion (ECAE) – Processed and Rolled AZ31 Magnesium Alloy Sheet

by Laszlo J Kecskes and Vincent H Hammond
Weapons and Materials Research Directorate, ARL

Michael Eichhorst, Lothar Meyer, and Norman Herzig
Nordmetall GmbH, Adorf-Neukirchen, Germany

REPORT DOCUMENTATION PAGE

Form Approved
OMB No. 0704-0188

1. REPORT DATE *(DD-MM-YYYY)*	2. REPORT TYPE	3. DATES COVERED (From - To)
April 2017	Technical Report	April 2015–January 2016

4. TITLE AND SUBTITLE
Quasi-Static and Dynamic Characterization of Equal Channel Angular Extrusion (ECAE) – Processed and Rolled AZ31 Magnesium Alloy Sheet

5a. CONTRACT NUMBER
W911NF-14-1-0517

5b. GRANT NUMBER

5c. PROGRAM ELEMENT NUMBER

6. AUTHOR(S)
Laszlo J Kecskes, Vincent H Hammond, Michael Eichhorst, Lothar Meyer, and Norman Herzig

5d. PROJECT NUMBER

5e. TASK NUMBER

5f. WORK UNIT NUMBER

7. PERFORMING ORGANIZATION NAME(S) AND ADDRESS(ES)
US Army Research Laboratory
ATTN: RDRL-WMM-F
Aberdeen Proving Ground, MD 21005-5069

8. PERFORMING ORGANIZATION REPORT NUMBER
ARL-TR-8006

9. SPONSORING/MONITORING AGENCY NAME(S) AND ADDRESS(ES)

10. SPONSOR/MONITOR'S ACRONYM(S)

11. SPONSOR/MONITOR'S REPORT NUMBER(S)

12. DISTRIBUTION/AVAILABILITY STATEMENT
Approved for public release; distribution is unlimited.

13. SUPPLEMENTARY NOTES

14. ABSTRACT
Previously, we developed a rolling schedule for Equal Channel Angular Extruded (ECAE) AZ31 magnesium (Mg) alloy plate material. Herein, we compare the room temperature quasi-static and dynamic mechanical properties of the as-ECAE processed plates (with textures A and C) to the subsequently rolled sheet material. Further, our investigation compares the batch-to-batch variation of 2 different lots of texture C plate material. Earlier results have shown that the plate material (especially texture A) exhibits anisotropic mechanical properties in the transverse and longitudinal directions. While to a large extent the initial ECAE process-induced banded microstructure is preserved after rolling, the property difference between the 2 directions is minimized. Closer examination of the sheet materials reveals a highly aligned microstructure along the rolling direction, consisting of fine sub-10-μm-sized Mg grains. Under dynamic loading conditions, both texture type sheet materials exhibit higher strengths, but lower ductility than at quasi-static testing conditions. The texture A sample was more ductile at the higher rates and yielded more consistent results than those obtained from the texture C sample.

15. SUBJECT TERMS
Mg, magnesium, ECAE, mechanical properties, equal channel angular extrusion, quasi-static, dynamic characterization

16. SECURITY CLASSIFICATION OF:			17. LIMITATION OF ABSTRACT	18. NUMBER OF PAGES	19a. NAME OF RESPONSIBLE PERSON
a. REPORT	b. ABSTRACT	c. THIS PAGE			Laszlo J Kecskes
Unclassified	Unclassified	Unclassified	UU	58	19b. TELEPHONE NUMBER (Include area code) 410-306-0811

Contents

List of Figures

List of Tables

Acknowledgments

Special kudos to Messrs. Gallaher and Runk for performing the equal channel angular extrusion processing of the AZ31B magnesium alloy plates and for the macrophotography of the plate and rolled sheet materials.

1. Introduction

Magnesium (Mg) and its alloys, with their low-mass densities, may offer new opportunities in many structural applications. For this reason, the US Army Research Laboratory (ARL) conducted a 5-year research program that developed high-strength Mg alloys through severe deformation processing methods. Although test results indicated that it is unlikely that Mg alloys will directly replace steel or aluminum as a monolithic armor material, it could be potentially used as a component in composite structures. With a density of about a quarter of steel, Mg may find a unique and/or niche utilization in applications such as personnel body armor where the reduction of mass and any type of weight savings is paramount, provided the ultrahigh-strength plates could be formed into thin sheets.

Because of its low melting point and good castability, many components made from Mg can be produced by casting. Unfortunately, such cast parts have poor mechanical properties, for example, low strength and ductility, and, therefore, cannot be used for many structural applications. Moreover, wrought Mg sheets or plates are very difficult to produce because of the intrinsically low room temperature ductility resulting from Mg's low-symmetry hexagonal close-packed crystal structure (basal slip only). However, the ductility of Mg can be increased significantly by increasing the processing temperature to approximately 300 °C. Unfortunately, despite the availability of alternative deformation mechanisms (prismatic and pyramidal slip and twinning), at or above this temperature, dynamic recrystallization processes take place that could negate the benefits of cold and warm working.

Previously, in ARL-TR-7644,[1] April 2016, we have reported good success with large-scale warm rolling of AZ31B Mg alloy plate material (15.24 × 15.24 × 1.27 cm) subjected to equal channel angular extrusion (ECAE). In that report, we described a possible sequence of rolling steps for reducing the initial plate thickness from about 9 to 1.5 mm without the introduction of significant grain growth or edge cracking in the rolled sheet material. It was determined that a rolling temperature of about 275 °C, with a degree of deformation of about 10% per rolling pass and a rolling speed of about 1 m/s was very promising. Moreover, the results indicated the importance of starting texture, as one set of the ECAE-processed plates proved less susceptible to edge cracking and thus yielded a more crack-free sheet product.

During extrusion, the ECAE plates were wrapped in a thin layer of Teflon sheathing to reduce frictional forces. However, the sheathing wrinkled, crinkled, flaked, or folded, causing the formation of a large number of surface and bulk defects in the Mg plate material. Although the affected layer was removed by surface milling

prior to the rolling experiments, it rendered the initial plates somewhat thinner than their nominal dimension of 12.7 mm. Since then, the use of Teflon was reevaluated and its attachment modified, which resulted in an overall improvement of the extrusion procedures. In turn, this also reduced the number of surface defects. As a result, the decision was made to demonstrate the applicability and reproducibility of this previously developed method with additional ECAE-processed plates with a starting thickness of 12.5 mm.

Additionally, before the onset of these second set of rolling experiments, the mechanical properties of one representative ECAE plate from this batch was measured and compared to the texture C plate results from the previous investigation. Furthermore, the tensile properties of 2 representative plates (namely A26 and C25) from each texture type, A and C, were measured at higher dynamic rates using a unique rotating wheel testing apparatus. This equipment, developed at Nordmetall, is capable of applying a tensile load at a rate of about 150 s^{-1}. These results were compared to those of the mechanical properties under quasi-static loading. As such, the influence of strain rate on the strength and ductility could be determined.

For extending the scope of the rolling experiments, the 6 new ECAE processed plates with a thickness of about 12.5 mm were shipped from ARL, Aberdeen Proving Ground, Maryland, to Nordmetall GmbH, Adorf-Neukirchen, Germany (Table 1). Macrophotography of the as-received plates are shown in Fig. 1. Even though the defects were reduced in number and size, cracks and surface imperfections, especially at the edges, can be still observed. The load versus displacement curves obtained during ECAE processing for each of the plates is presented in the Appendix. These curves are very useful in identifying any type of premature or nonuniform deformation (e.g., shear localization and failure) in the extruded material.

Table 1 Overview of the new as-received ECAE-processed plates (all texture C)

Description	Thickness (mm)	Width (mm)	Length (mm)
Plate 61	~12.5	~153	~128
Plate 62	~12.5	~153	~128
Plate 63	~12.5	~153	~128
Plate 65	~12.5	~153	~128
Plate 66	~12.5	~153	~128
Plate 67	~12.5	~153	~128

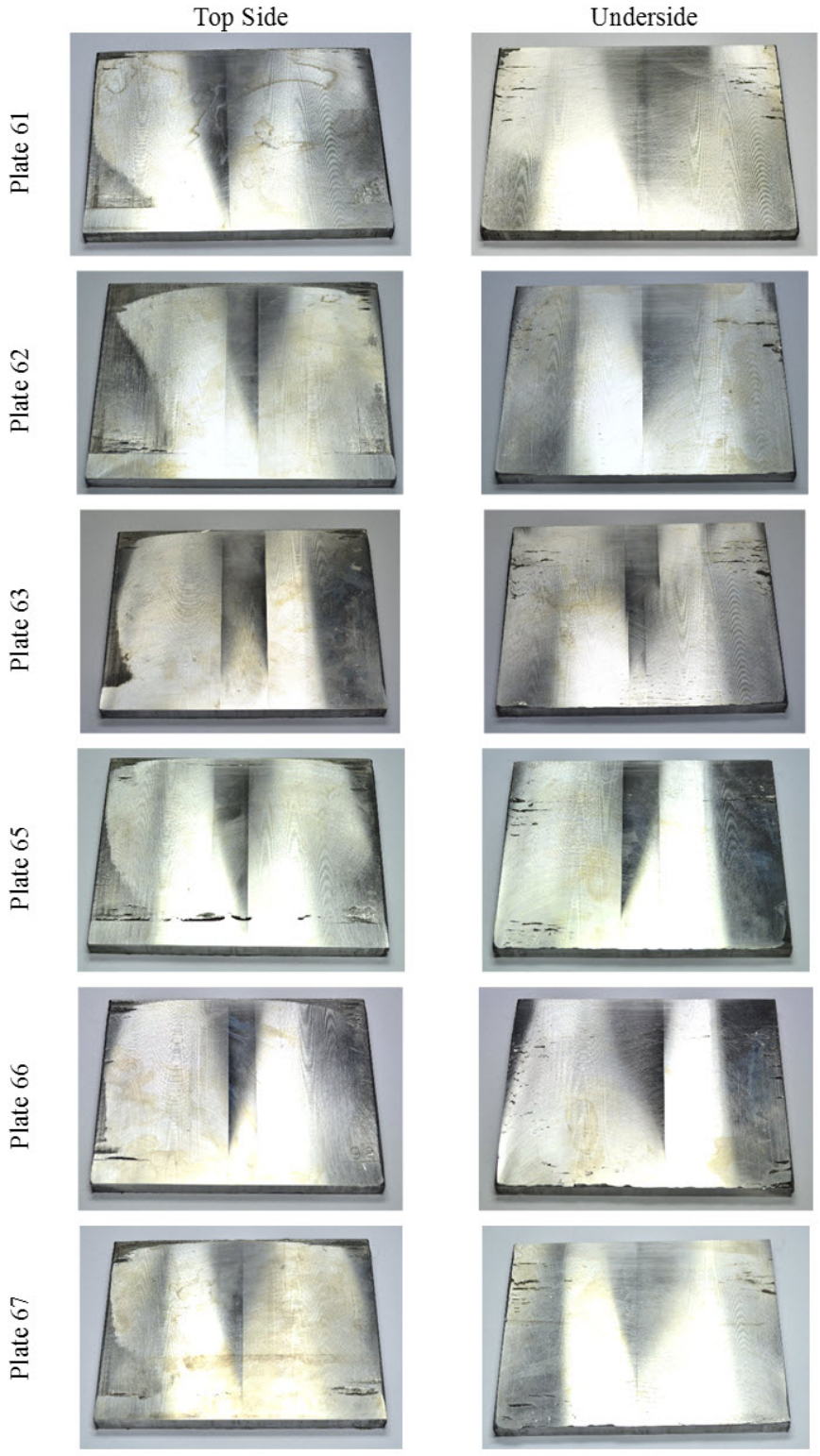

Fig. 1 Macrophotography of the as-received ECAE-processed Mg plate material

2. Experimental Procedures

2.1 Extrusion Procedures

To develop the appropriate post-ECAE C texture type in the plates, similar procedures as those used in the previous trials were adopted in this study.[1] Briefly, these entailed sectioning the 15.24- × 15.24- × 1.27-cm (6- × 6- × 0.5-inch) plates from a large block of AZ31B tooling plate material, then extruding each plate for a total of 6 passes, consisting of 2 A passes at 225 °C; 2 C passes at 200 °C; and 2 C passes at 150 °C. For route A there is no rotation of the plate between passes; for route C, the plate is rotated by 180° around the plate normal before the next pass. An exception to the previously used procedures was that Plates 61–67 were sectioned in a different orientation from the tooling plate (Fig. 2). Previously, the orientation of the plate normal in the extruded and tooling plates was parallel. As such, during the subsequent ECAE processing, the extrusions essentially took place in the rolling direction. In the current extrusions, the orientation of the extruded plate normal was perpendicular to that of the tooling plate. That is, the extrusion took place in the transverse direction. This orientation was more favorable for producing crack-free plate material on the first pass.

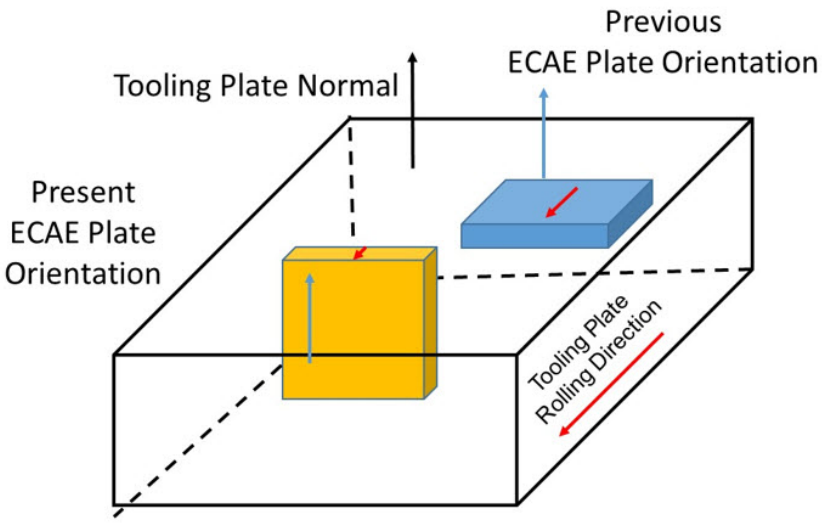

Fig. 2 Relationship between the tooling plate and the ECAE plate orientations

2.2 Metallographic Sample Preparation

The microstructure of the ECAE processed AZ31 material was investigated in the as ECAE and as-rolled condition. Representative specimens were taken from the transverse and longitudinal directions of Plate 61 (Fig. 3). The specimens were

mounted in an epoxy resin and prepared using conventional metallographic techniques. A final etching, using diluted picric acid, was used to better reveal the underlying grain structure.

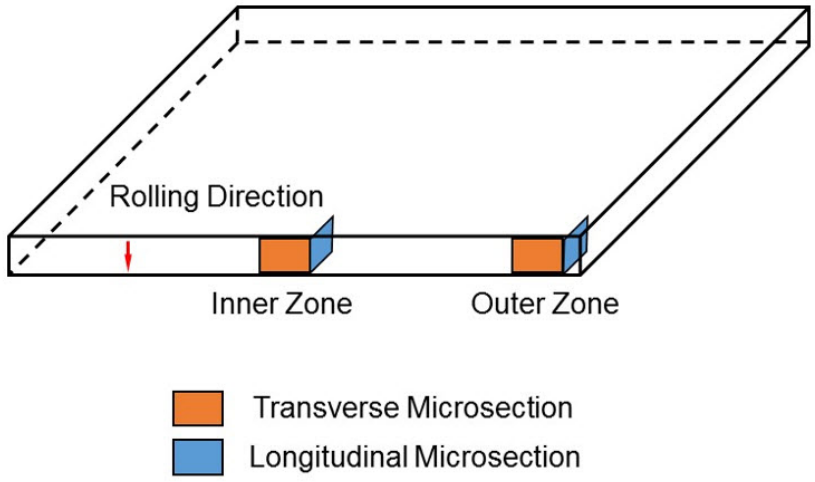

Fig. 3 Microsection positions of the as-received plates

2.3 Hot Rolling Procedures

The rolling experiments were performed in cooperation with the Technical University Bergakademie Freiberg, a leading university in Germany for the production of Mg sheet materials. After preheating, the initially 12.5-mm-thick plates were rolled to a thickness of about 1.5 mm. The hot rolling was performed on a dual rolling mill (Hugo Sack Mills, formerly of Dusseldorf, Germany) (Fig. 4). The diameter of the roller was about 360 mm, with a maximum rolling force of 2400 kN. The rollers are driven by a 160-kW electric motor capable of producing a torque of 30 kN·m. The rollers were preheated to about 120 °C with electric blankets before the rolling experiments, and a lubricant was sprayed on the rollers before each rolling pass. The rolling speed was about 1 m/s, a common rolling speed for AZ31.

Fig. 4 Rolling mill (Hugo Sack GmbH)

The preheating (about 30 min at 275 °C) and intermediate annealing between the rolling steps (about 15 to 20 min at 275 °C) was performed in a convection air furnace (Fig. 5). A homogenization annealing treatment was not performed before the start of the rolling experiments.

Fig. 5 Convection air furnace

The rolling experiments started with preheating the plates at about 275 °C for about 30 min in the convection air furnace followed by 18 rolling passes and 17 intermediate annealing treatment steps (Table 2). As the table illustrates, the degree of deformation for every rolling pass was about 10% for the first 15 rolling passes. Because of the previously positive experience with increasing the extent of deformation for the last rolling passes, the degree of deformation for the last 3 steps was increased to about 20%. Compared with the procedures described in ARL-TR-7644,[1] more rolling passes were necessary in these experiments. This was a direct consequence of the greater initial thickness of the as-received plate material. To prevent and minimize further crack growth, after every rolling pass an intermediate annealing at a temperature of 275 °C for 15 to 20 min was performed.

Table 2 Overview of the rolling passes

Rolling Pass	Material Thickness [mm]	Degree of Deformation [%]
Initial	12.5	NA
1	11.4	8.8
2	10.4	8.8
3	9.5	8.7
4	8.7	8.4
5	7.9	9.2
6	7.2	8.9
7	6.6	8.3
8	6.0	9.1
9	5.5	8.3
10	5.0	9.1
11	4.4	12.0
12	4.0	9.1
13	3.6	10.0
14	3.2	11.1
15	2.9	9.4
16	2.4	17.2
17	1.9	20.8
18	1.5	21.1

2.4 Quasi-Static Tensile Tests

The mechanical properties of the as-received plates were determined using quasi-static tensile tests at room temperature and strain rates of about 10^{-3} s^{-1}. Small sections of Plate 61 were cut off for fabricating the tensile specimens in both the longitudinal and transverse directions relative to the extrusion direction. The tensile specimen geometry and pertinent dimensions are shown in Fig. 6. The gage length was about 10.5 mm.

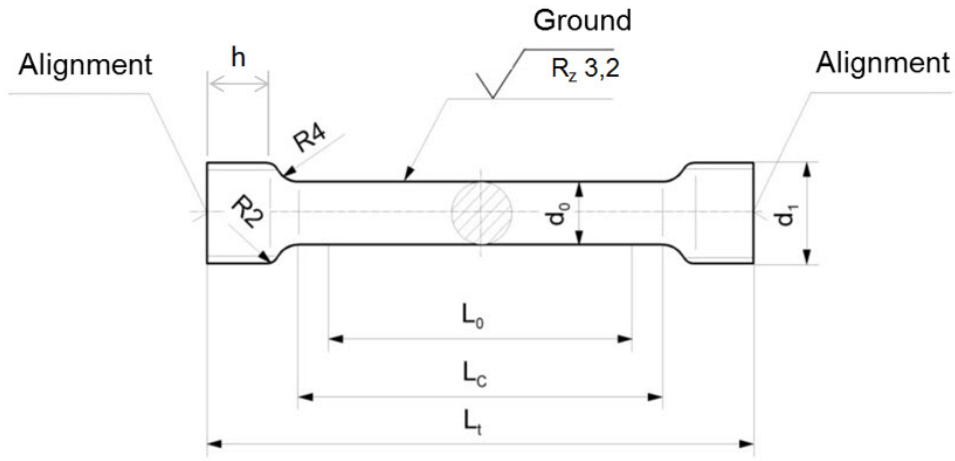

d_0	L_0	d_1	h_{min}	L_c	L_t
3.56 $^{\pm 0.01}$	10.5	M6 (6 mm thread)	17	14	60*

Fig. 6 Tensile specimen geometry and dimensions in millimeters (as-received ECAE material)

The tensile tests were performed using a universal testing machine (Zwick/Roell Company GmbH, Ulm, Germany). The maximum force of the testing machine is 100 kN and the testing velocity can be varied between 0 mm/min and 500 mm/min. The experimental setup, including the load frame, is shown schematically in Fig. 7. The testing load frame consists of a stiff frame, 2 ball bearing screw spindles, and a crosshead connected with the ball bearing screw spindles. The forces were measured with a load cell with a maximum force of 5 kN. The specimen elongation was measured with a fine displacement extensometer.

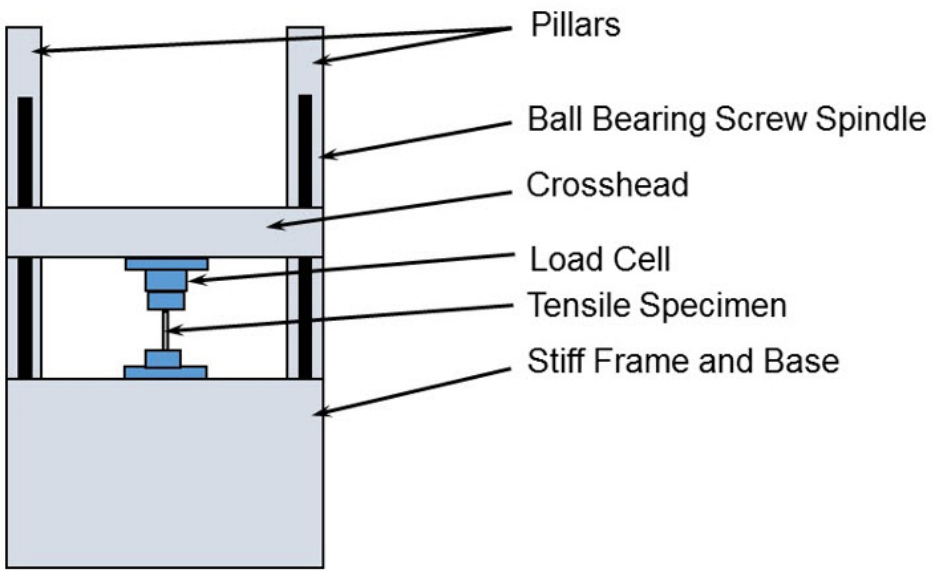

Fig. 7 Universal testing machine (schematic)

2.5 Dynamic Tensile Tests

The mechanical properties of the as-rolled ECAE processed material was investigated by dynamic tensile tests at room temperature and strain rates of about 150 s^{-1}. The tensile specimen geometry is shown in Fig. 8. The gage length is about 9 mm and the test specimen width about 3 mm. The specimen thickness was about 1.5 to 1.65 mm. Again, representative specimens were taken along the longitudinal and transverse directions relative to the rolling direction.

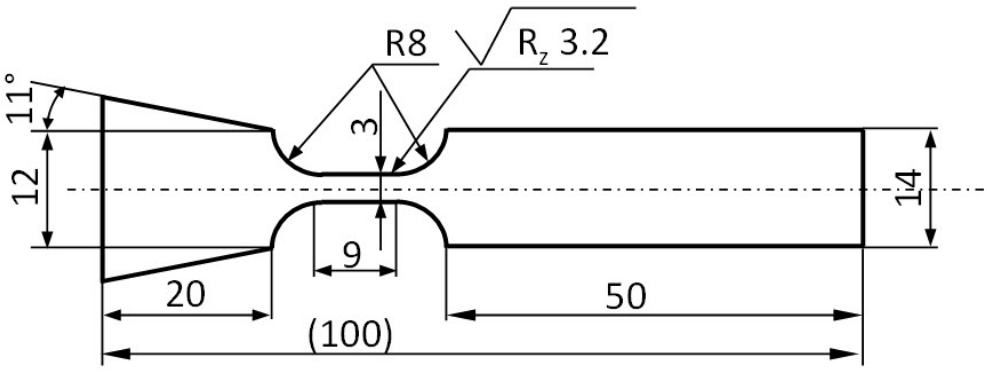

Fig. 8 Tensile specimen geometry (dimensions in millimeters)

The tensile tests at high strain rates of about 150 s^{-1} were performed using a rotating wheel machine. The rotating wheel machine, Figs. 9 and 10, is employed for tensile test velocities from 1 m/s up to about 40 m/s. It consists of a test frame stand, motor, and a large flywheel (220 kg) with a retractable claw. Figure 10 shows the claw

unlocked, then released at the required rotational test velocity and, after its release, it contacts the yoke (or bottom) of a stationary sample holder. As the extended claw contacts and engages this yoke, it pulls on the test specimen, which is held in the holder. The force measurement is obtained from strain gages attached to the specimen. Assuming that the Young's modulus is independent of the strain rate, the stress can be calculated from the strain gage signals and the cross sectional area of the specimen.

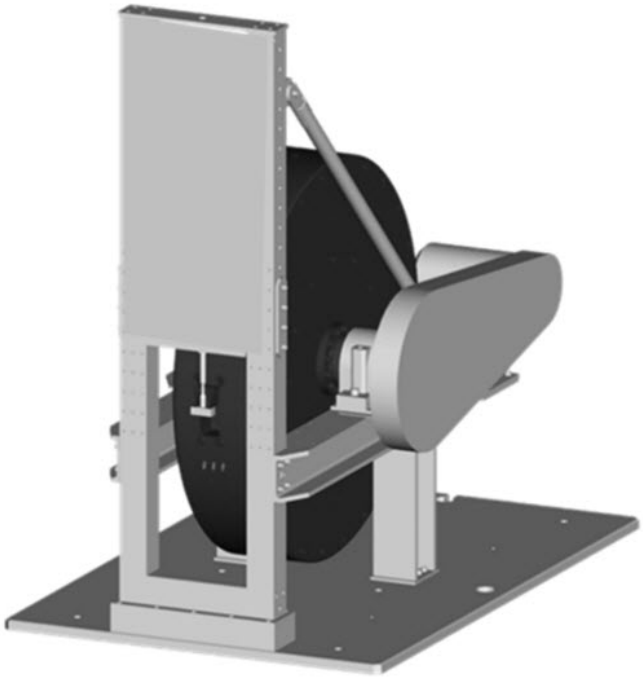

Fig. 9 Nordmetall's rotating wheel machine (schematic)

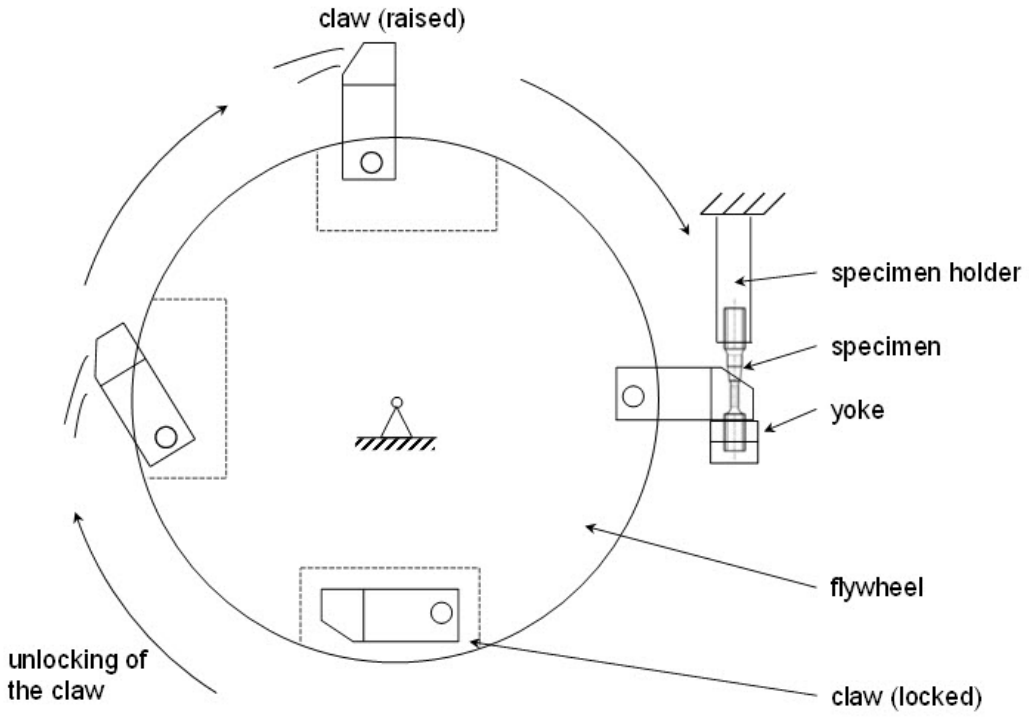

Fig. 10 Rotating wheel machine illustrating the various stages of operation: claw release, claw extension, contact and engagement of the specimen, and retraction

Because of the high-rotational energy capacity of this apparatus compared to the energy consumed during the impact, it is reasonable to assume that the test velocity is nearly constant up to the failure of the sample, even for materials with high strength and high ductility. As such, to determine precise yield stress values, the strain gages were attached to the gage length to measure the elastic deformation strains as well as a part of the plastic deformation up to about 2% or 3%. For larger plastic deformations, the strain measurements were carried out using an electro-optical extensometer with a bandwidth of 400 kHz.

3. Results and Discussion

3.1 Microstructural Examination of the As-Received ECAE Plate Material

Microsections in the longitudinal and transverse directions of Plate 61 were prepared from the as-received ECAE material. Figure 11 shows typical microsections of the inner and outer zones. The appearance of these sections are very similar to those of the initially processed texture C plates.[1] The difference in initial plate orientations did not have a significant effect on the microstructure

evolution. Further, if the inner and outer zones of the plate are compared to each other, the microstructures are found to be very similar. The bulk of the ECAE material exhibits a very fine microstructure that could not be thoroughly investigated by optical microscopy alone. In addition to the clearly visible macroscale features such as the deformation bands, some of the finer scale microstructure is not easily discernible at these magnifications. However, the optical images are of sufficiently good quality to distinguish between the regions of smaller and larger grains with a diameter of about 50 µm. This is especially prominent in the longitudinal microsections; the series of shear bands with an angle of about 45° relative to the ECAE extrusion processing direction can be observed. There is extensive deformation in these regions. It is reasonable to attribute this shearing and the appearance of these shear bands to the nature of the ECAE processing route and active deformation mechanisms at the step-down extrusion temperatures. In the transverse microsections, there is extensive deformation but without the 45° tilt relative to the extrusion direction. Furthermore, small and large precipitate structures were observed in all microsections. While necessary to fully describe the as-extruded microstructure, the more detailed examination of these structures by scanning electron microscopy (SEM) and energy dispersive X-ray analysis will be deferred to a subsequent study.

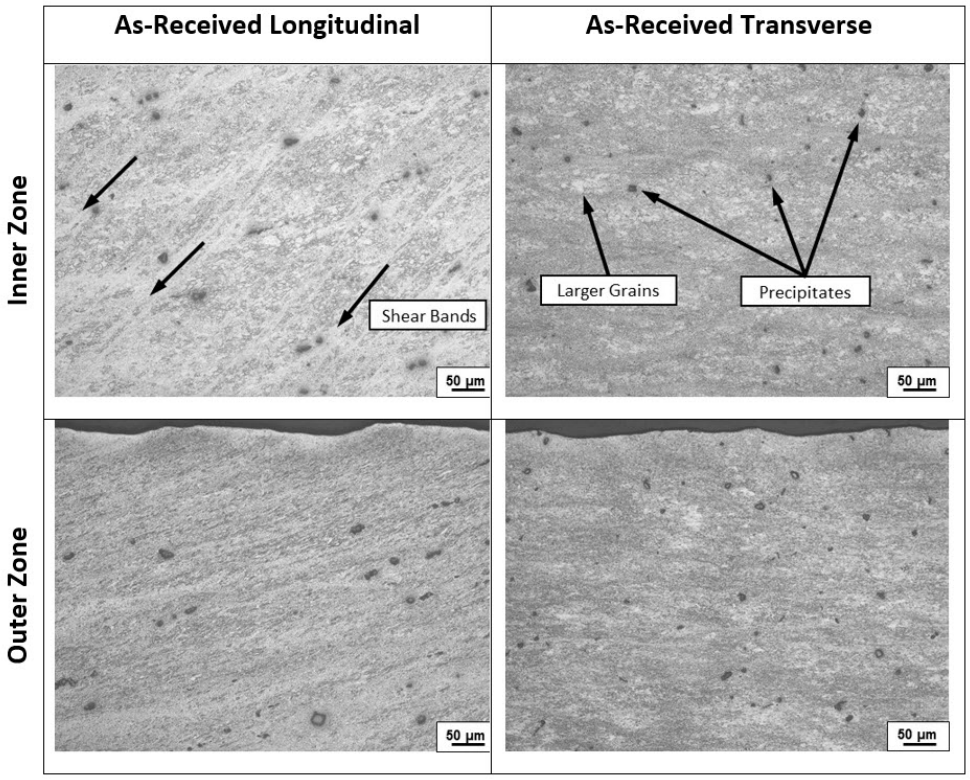

Fig. 11 Microsections of the as-received ECAE Plate 61 (texture C)

3.2 Hot Rolling of the Plates

In general, the surface quality of the plates produced for this study was considerably better than those of the previously supplied plates.[1] However, the plates were still characterized by small edge cracks transverse to the extrusion direction on the underside of the plates (see Fig. 1).

The rolling experiments started with a preheating the plates to 275 °C for about 30 min in the convection air furnace followed by 18 rolling passes and 17 intermediate annealing steps for about 15 to 20 min at 275 °C (see Table 2 for the rolling schedule). Good rolling results were obtained when 18 rolling passes were used to attain a thickness of about 1.5 mm. Only small edge cracks could be observed for all of the rolled sheets (see Fig. 12). The reason for these cracks could be traced to extrusion-induced defects in the as-received original plate material. These small transverse cracks remained in each of the sheets after each rolling pass, however, without significant growth. As such, the crack lengths at the edges of the final as-rolled sheets varied between 5 and 25 mm, leaving a crack-free width of about 120 to 130 mm. Figures 13–18 show that the extent of the damaged region varied from sheet to sheet.

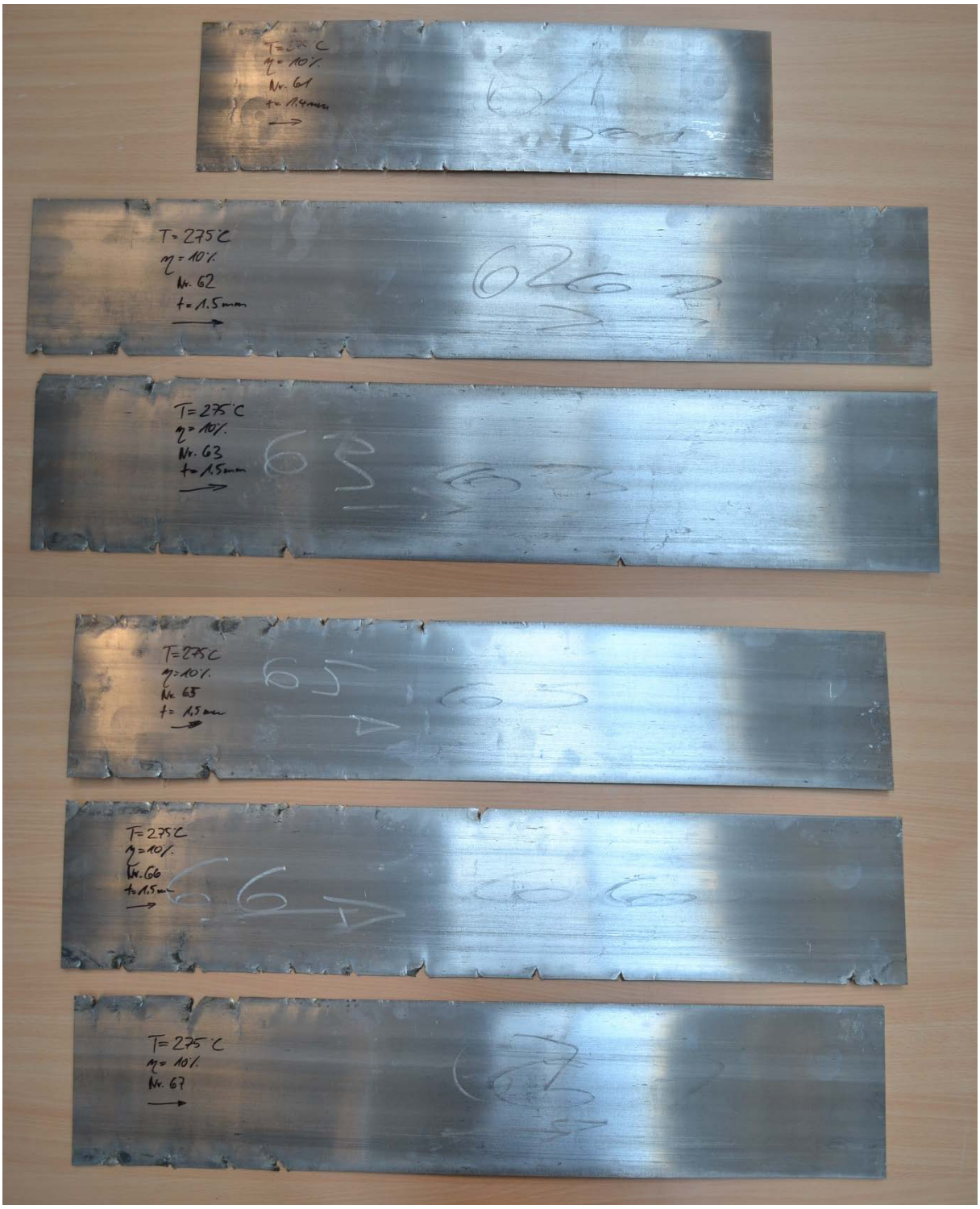

Fig. 12 Macrophotograph of the 6 rolled sheets; from top to the bottom of the photograph the sheets are placed sequentially from 61, 62, 63, 65, 66, and 67 (texture C, rolling T = 275 °C, 18 rolling passes, final thickness, t = 1.5 mm)

Fig. 13 Enlarged view of the edge cracks for sheet 61; typically, damage was limited with crack lengths of about 5 to 15 mm

Fig. 14 Enlarged view of the edge cracks for sheet 62; typically, damage was limited with crack lengths of about 5 to 15 mm

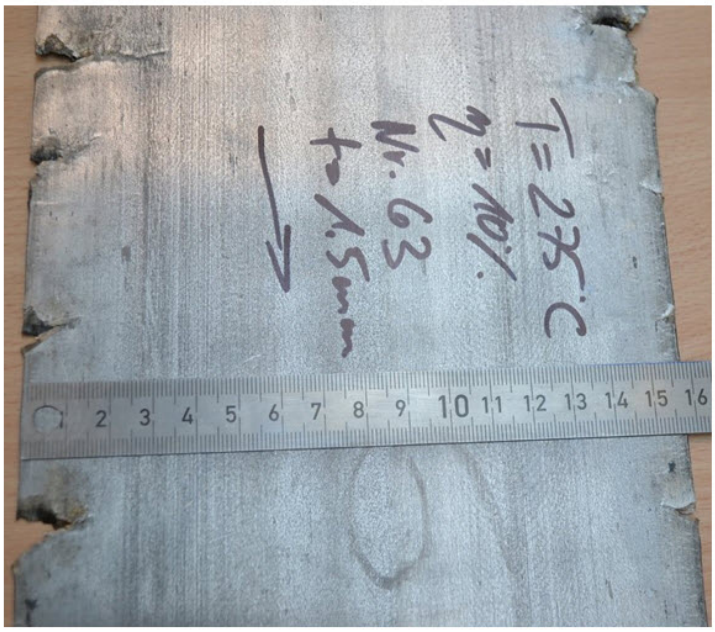

Fig. 15 Enlarged view of the edge cracks for sheet 63; typically, damage was limited with crack lengths of about 5 to 25 mm

Fig. 16 Enlarged view of the edge cracks for sheet 65; typically, damage was limited with crack lengths of about 5 to 25 mm

Fig. 17 Enlarged view of the edge cracks for sheet 66; typically, damage was limited with crack lengths of about 10 to 25 mm

Fig. 18 Enlarged view of the edge cracks for sheet 67; typically, damage was limited with crack lengths of about 10 to 25 mm

3.3 Microstructural Examination of the Rolled Sheets

After rolling to a thickness of about 1.5 mm, the microstructure of the sheet materials was investigated at their respective inner and outer regions. As was done for the as-received plate material, representative microsections were taken in both the longitudinal and transverse orientations.

After rolling, larger areas, with a much higher degree of deformation, are observed for all sheets. The microstructure is highly heterogeneous, with alternating coarse- and fine-grained regions. This heterogeneity likely carried through from the ECAE process. However, the more refined microstructure containing very fine grains (Fig. 19) is likely determined by further recrystallization processes that occurred during rolling. Also, note the more prominent alignment of the precipitate colonies and substructures in the rolling plane (longitudinal) direction between the zones of small and large deformation. Occasionally, larger grains with about a 10-µm grain size are found. In the regions with larger grains, small twins are observed, which were formed due to the relatively low rolling temperature and high-deformation degree.

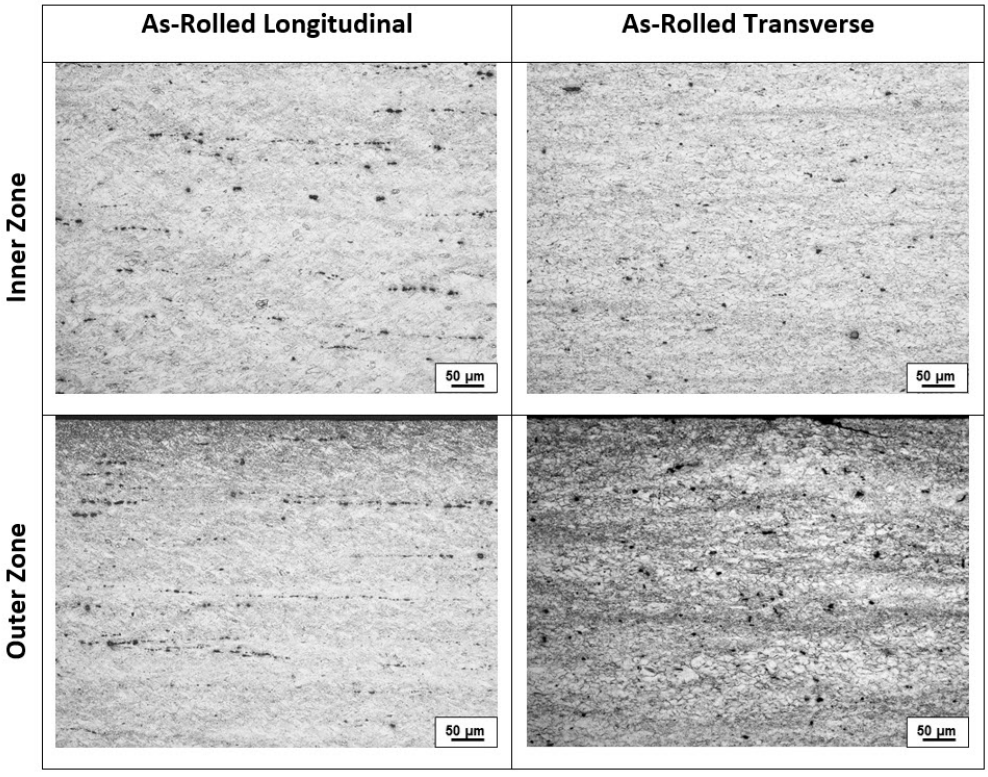

Fig. 19 Microsections of as-rolled Plate 62 (texture C, t = 1.5 mm)

3.4 Comparison of Unprocessed and ECAE-Processed Sheet Materials (Batch 1, per ARL-TR-7644)[1]

In Figs. 20 and 21, bar graphs summarizing the longitudinal and transverse quasi-static tensile properties of rolled AZ31 sheets obtained from a conventional supplier and the ECAE material produced for this study are compared. The properties of the rolled sheet 3.2 (without prior ECAE processing), which was evaluated previously and reported in ARL-TR-7644,[1] were included for comparison with the properties of the ECAE processed sheets of A26 and C25. Sheet 3.2 was rolled at 425 °C, for a total of 8 rolling passes to a thickness of less than 1.5 mm. An equivalent sheet, 3.1, was subjected to a final anneal treatment at 330 °C for 30 min; this annealing step caused a roughly 10% decrease in strength, but a concurrent increase in ductility. The former temperature is considerably higher than the recent minimum of 275 °C obtained through optimization of the rolling conditions described herein. Unlike the specimen geometry shown in Fig. 6, all of these tensile property investigations were performed using a slightly different flat specimen geometry (l_0 = 15 mm, w = 5 mm, and t = 1.5–1.65 mm). The stress-strain tests were conducted at a nominal strain rate of 10^{-3} s^{-1} and at room temperature. The stress-strain diagrams for sheets 3.1, 3.2, A26, and C25 are provided in the Appendix.

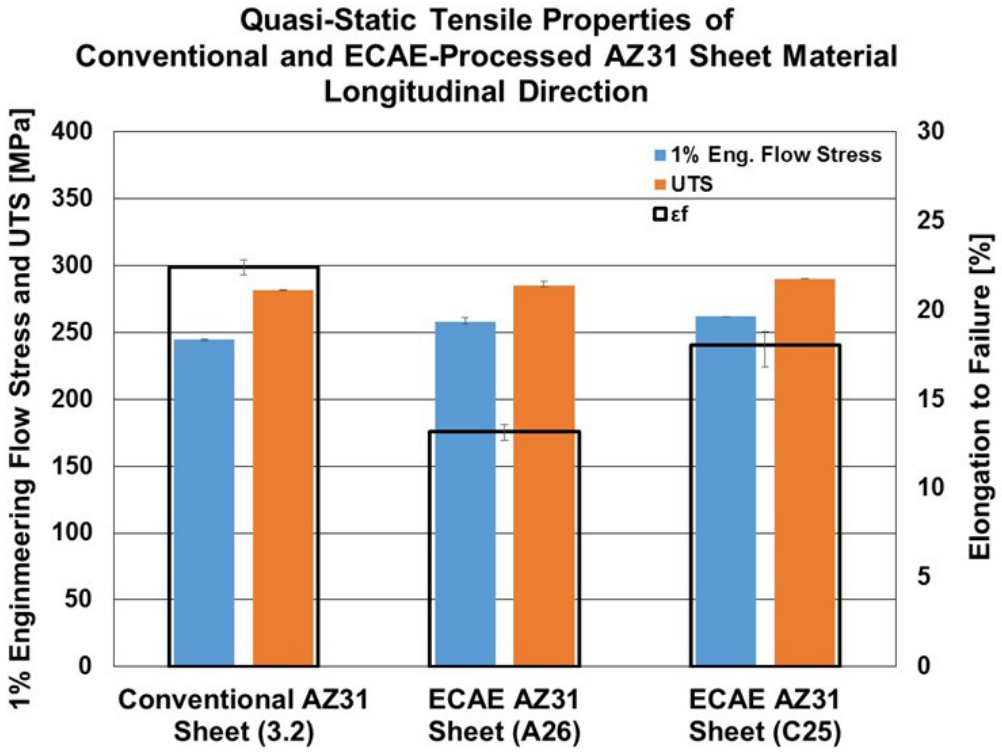

Fig. 20 Quasi-static tensile properties of conventional and ECAE-processed AZ31 sheet material in the longitudinal direction

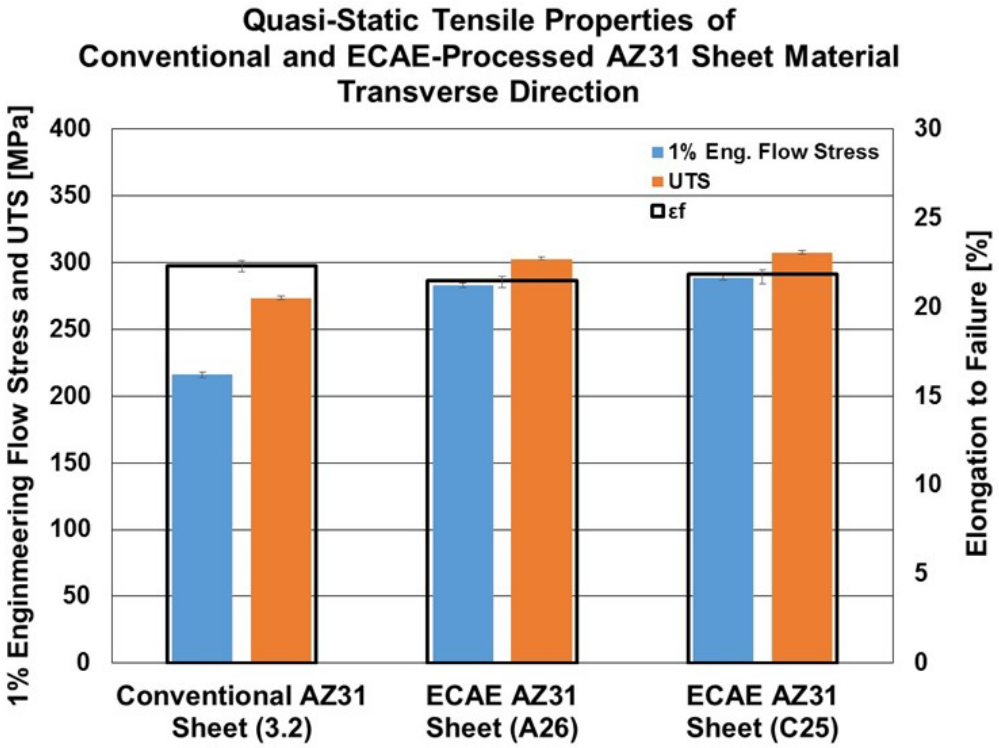

Fig. 21 Quasi-static tensile properties of conventional and ECAE-processed AZ31 sheet material in the transverse direction

A more detailed review of the prior results indicates that the transverse and longitudinal strength levels are about the same for the texture A plate material. However, the ductility in the latter direction is lower. In comparison, in the texture C plate, the longitudinal strength level is considerably lower, while the ductility in the 2 directions is more uniform. After rolling, both texture types have similar final strength levels, but during rolling, the preexisting and retained anisotropy (or asymmetry) in ductility causes the texture A plate to develop cracking. Thus, the more uniform ductility of the texture C plate material allows it to be processed more easily. In other words, the rolling process improves the strength of the materials, most likely, due to grain size refinement via recrystallization, but without affecting the initial ductility. That is, in the texture A plates, the inherent lower ductility in the longitudinal direction hinders further processing.

Compared with the conventional AZ31 sheet, the elongation to failure values in the rolled texture A and C sheets (A26 and C25, respectively) decrease, indicative of the fact that the preferential alignment of the grains and potentially the precipitates along the rolling direction may not be necessarily advantageous. However, in the transverse direction, this alignment does not affect the benefits gained from the increase in the flow stress and ultimate tensile strength.

Table 3 lists the average values of the 0.5% and 1.% engineering flow stress, ultimate tensile stress (UTS), elongation to failure, ε_f, and reduction of area (i.e., necking to failure), q. For the conventional AZ31 sheet 3.2, the stress and strain values listed are an average of 2 tests; whereas, for the 2 ECAE processed sheets (textures A and C, respectively), the stress and strain values listed are an average of 3 tests.

Table 3 Quasi-static tensile test results for AZ31 rolled sheet types with and without prior ECAE processing

Quasi-Static Tensile Test Results							
Specimen	**Temperature**	**Strain Rate**	**0.5% Engineering Flow Stress**	**1% Engineering Flow Stress**	**UTS**	**ε_f**	**q**
	[°C]	**[s^{-1}]**	**[MPa]**	**[MPa]**	**[MPa]**	**[%]**	**[%]**
Longitudinal							
Conventional AZ31 Sheet (3.2)	RT	10^{-3}	238	245	282	22.4	32.65
ECAE AZ31 Sheet (A26)	RT	10^{-3}	247	258	285	13.2	16.2
ECAE AZ31 Sheet (C25)	RT	10^{-3}	253	262	290	18.0	23.4
Transverse							
Conventional AZ31 Sheet (3.2)	RT	10^{-3}	210	216	274	22.3	14.85
ECAE AZ31 Sheet (A26)	RT	10^{-3}	277	283	303	21.5	41.8
ECAE AZ31 Sheet (C25)	RT	10^{-3}	284	288	307	21.8	37.0

Notes: UTS = ultimate tensile stress; ε_f = elongation to failure; and q = reduction of area (necking to failure); RT = room temperature

Examination of the data in the figures and Table 3 indicates that in the longitudinal direction there is a slight increase in the strength of the ECAE processed material compared to the conventional sheet material. However, the elongation to failure decreases for both texture types. If the conventional material with a ε_f value of 22.4% is compared with the ECAE processed materials, with ε_f values of 13.2% for A26 and 18.0% for C25, the decrease is quite significant, especially for the texture A sheet.

Unlike the similar properties in the longitudinal direction, a comparison of the mechanical properties in the transverse direction indicates that there is a fairly large increase of about 70 MPa or 30% in the 1% flow stress and a notable increase of about 30 MPa or 11% in the UTS for the ECAE processed materials relative to the

conventional material. Also, the hardening is greater, especially in the conventional material. The elongation to failure remains nearly constant at about 22% between the various texture types. However, the differences in the necking to failure, 14.9% versus 41.8% and 37.0%, respectively, are significant and indicative that the conventional Mg alloy is more brittle than either ECAE processed sheet.

As was noted previously, there is a definite positive effect of ECAE processing on the mechanical properties; however, these benefits to improvements in ductility can be observed in the transverse, but not in the longitudinal direction. In part, this is attributed to a strong basal texture that develops during the extrusion sequence, which seems to be more pronounced in the longitudinal (extrusion) direction with increasing shear deformation with each pass using texture A, but not as much with texture C. During ECAE processing, using route C, on every second pass the sheared material is sheared back to its "unsheared" state. This action likely helps returning the microstructure of the grains to a more equiaxed morphology but without changing the preferential basal texture. Furthermore, because there is minimal shearing in the transverse direction, the effect of route A versus route C is not as pronounced. Lastly, these results are only for uniaxial tensile loading of the sheet materials. The performance of the different sheet materials should be investigated in the through thickness direction or under multiaxial loading conditions.

3.5 Quasi-Static Tensile Tests of the Recent Batch 2 of ECAE-Processed Material

The results of the quasi-static tensile tests from a plate recently produced for this study by ECAE processing (texture C, Plate 61) are illustrated in Fig. 22. Similar to what was observed before in the Batch 1 texture C plates,[1] compared with the unprocessed plate material, there is a significant increase in strength and good ductility in the transverse direction. The strength in the longitudinal direction is approximately one-half of that measured for the transverse direction. If the microstructures in the 2 orientations of the plate are compared, it is conceivable that the relative weakness in the longitudinal direction could be a result of the highly heterogeneous striated substructure consisting of alternating layers of refined and unrefined grains, partitioned by shear bands. This was also observed for the texture C plates from Batch 1. Regardless, the ductility of this plate from Batch 2 is considerably better than that obtained from the Batch 1 plates. Additionally, the shapes of the stress-strain curves are slightly different.

Specifically, for Plate 13, the transverse stress-strain curve is flatter, but the maximum strength is slightly higher, but at the expense of a lower ductility.(See the stress-strain curve for Plate 13 in the Appendix, Fig. A-11). Aside from the somewhat larger ductility, the differences in the longitudinal stress-strain curves are minimal between the 2 batches.

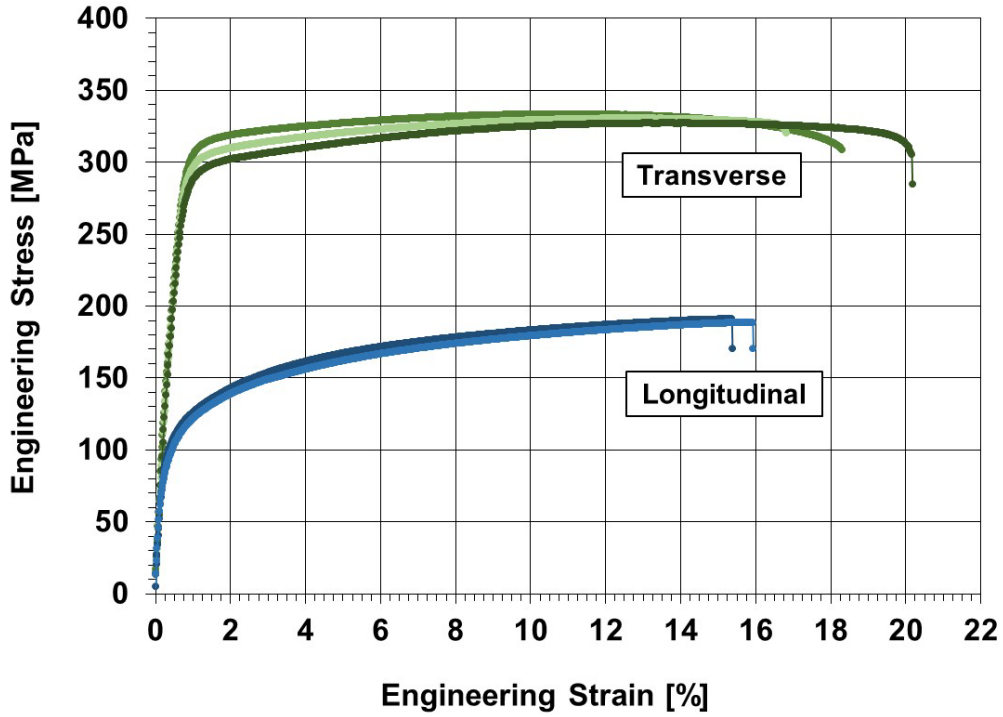

Fig. 22 Engineering stress–engineering strain diagram for ECAE processed Plate 61

A direct and quantitative comparison of the mechanical properties can be gleaned from the bar graphs shown in Figs. 23 and 24, with the average values from 3 tests listed in Table 4. If the 1% engineering flow stress and the UTS of Plate 61 (Batch 2) are compared to Plate 13 (Batch 1)[1], nearly similar strength values can be observed in the longitudinal direction (Fig. 23). However, in the transverse direction, a slightly decreased 1% flow stress and UTS can be observed for Plate 61. Interestingly, for Plate 61, in both directions, an increased elongation to fracture and reduction in area were determined (Fig. 24). However, a fairly large scatter exists in these data for the ε_f and q values in both batches of plate material, as indicated by the magnitude of the error bars. Regardless, because of its better ductility, it may be expected that the plates from Batch 2 are more easily deformed; that is, its rollability will be the same or better than that of Batch 1.

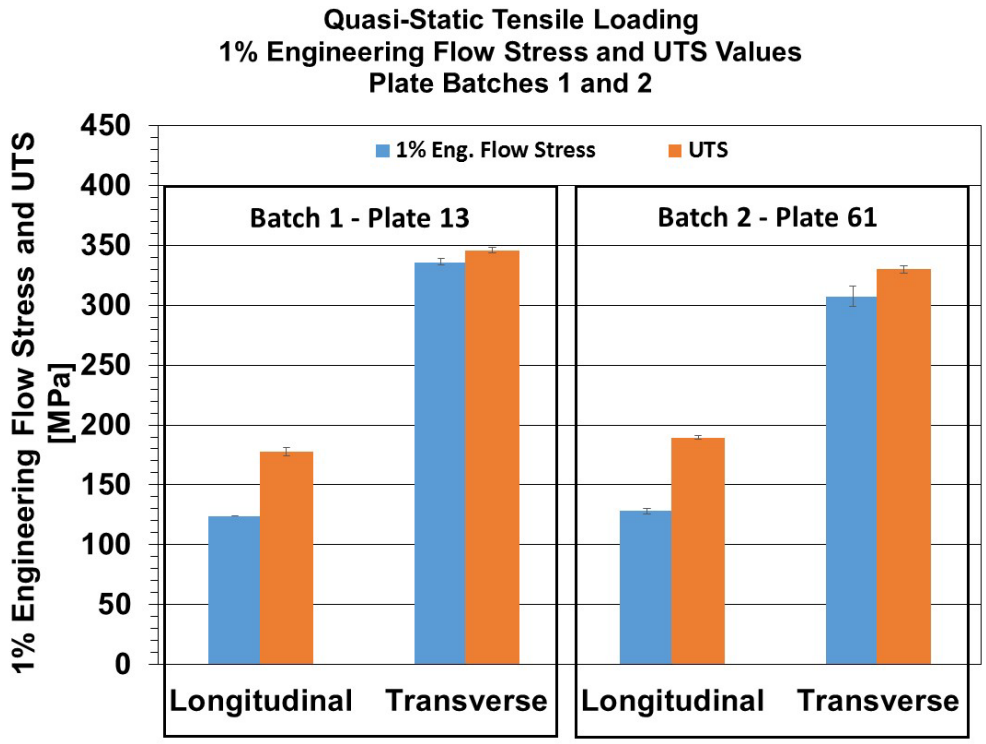

Fig. 23 Comparison of the 1% flow stress and UTS from the 2 batches of ECAE processed plates

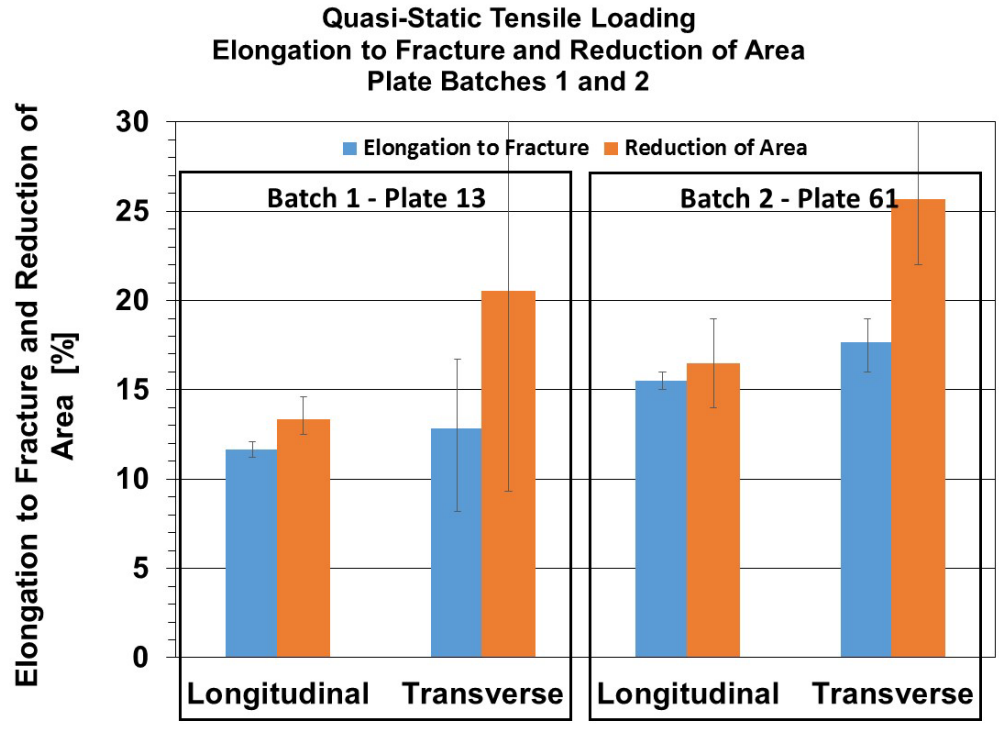

Fig. 24 Comparison of elongation to fracture and reduction of area from the 2 batches of ECAE processed plates

Table 4 Quasi-static tensile test results for AZ31 plates after ECAE processing

Quasi-Static Tensile Test Results						
Comparison of Plate Batch Properties - Texture C						
Temperature	Strain Rate	0.5% Engineering Flow Stress	1% Engineering Flow Stress	UTS	ε_f	q
[°C]	[s^{-1}]	[MPa]	[MPa]	[MPa]	[%]	[%]
Plate 13						
Longitudinal						
RT	10^{-3}	114	124	178	11.6	13.4
Transverse						
RT	10^{-3}	324	336	346	12.8	20.6
Plate 61						
Longitudinal						
RT	10^{-3}	116	128	190	15.5	16.5
Transverse						
RT	10^{-3}	299	307	330	17.7	25.7

Notes: UTS = ultimate tensile stress; ε_f = elongation to failure; and q = reduction of area (necking to failure); RT = room temperature

Subsequent to these comparative tests, the plates from Batch 2 were rolled into sheets and returned to ARL for further processing and incorporation into the target configuration. No further testing was performed on the as-rolled sheets from Batch 2. However, much like that observed for the previous texture C plates, it was expected that upon rolling the sheets would develop a more uniform strength profile. That is, the postrolled longitudinal direction strength was expected to increase to roughly match that in the transverse direction. However, the elongation to failure in the former direction was expected to remain lower than that in the latter direction.

3.6 Dynamic Tensile Properties of Rolled Mg Sheets

As part of the overall experimental program, the mechanical properties under dynamic loading conditions were also determined for the 2 texture types. Representative samples from each of the 2 texture types, namely from sheets A26 and C25 (see Fig. 25 for the characteristics of the sheets; note the better appearance of the texture C sheet) were taken. Plate A26 was ECAE processed to develop a texture A, and Plate C25 was ECAE processed to develop a texture C. These routes were described in more detail in ARL-TR-7644.[1] Both plates were rolled at a rolling temperature of 275 °C, with a degree of deformation of about 10% per rolling pass. The final thickness of both sheets was about 1.5 to 1.6 mm and the rolling speed was about 1 m/s.

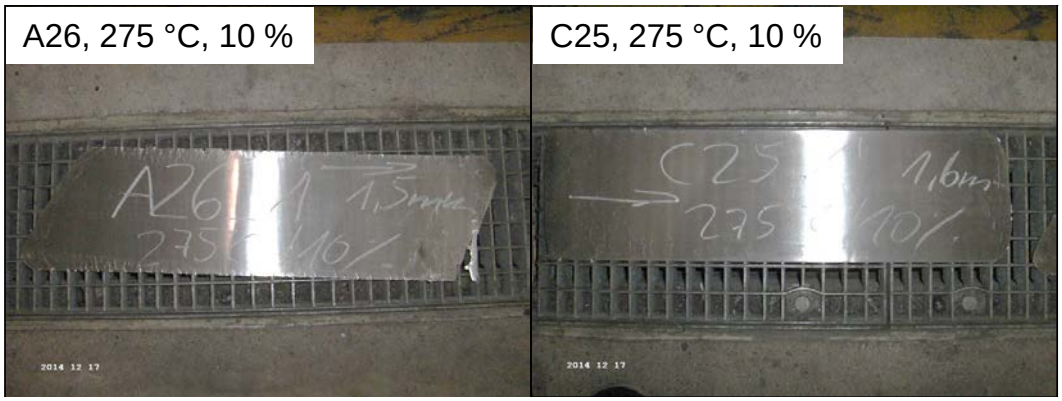

Fig. 25 Macrophotographs of the A26 and C25 sheets, respectively

The results of the dynamic tensile tests at strain rates of about 150 s^{-1} are shown in Figs. 26 and 27. Both sets of results show increased strength and ductility. More specifically, the increase in strength and the significant increase in ductility are greater in the transverse direction, as can be observed compared with that in the longitudinal direction for the A26 sheet. Similar to the A26 sheet, there is an increased strength in the transverse direction compared to the longitudinal direction for the C25 sheet. Despite attempts to carefully select and extract the dynamic tensile specimens from crack-free areas there are significant deviations in the stress-strain behavior from repeated tests for various specimens in the same orientations. This is especially the case for the C25 sheet results. These deviations could be explained by the presence of microcracks or failure zones induced in the microstructure of the material during roll processing. The mechanical properties of the A26 and C25 sheets under dynamic tensile loading conditions are summarized in Table 5.

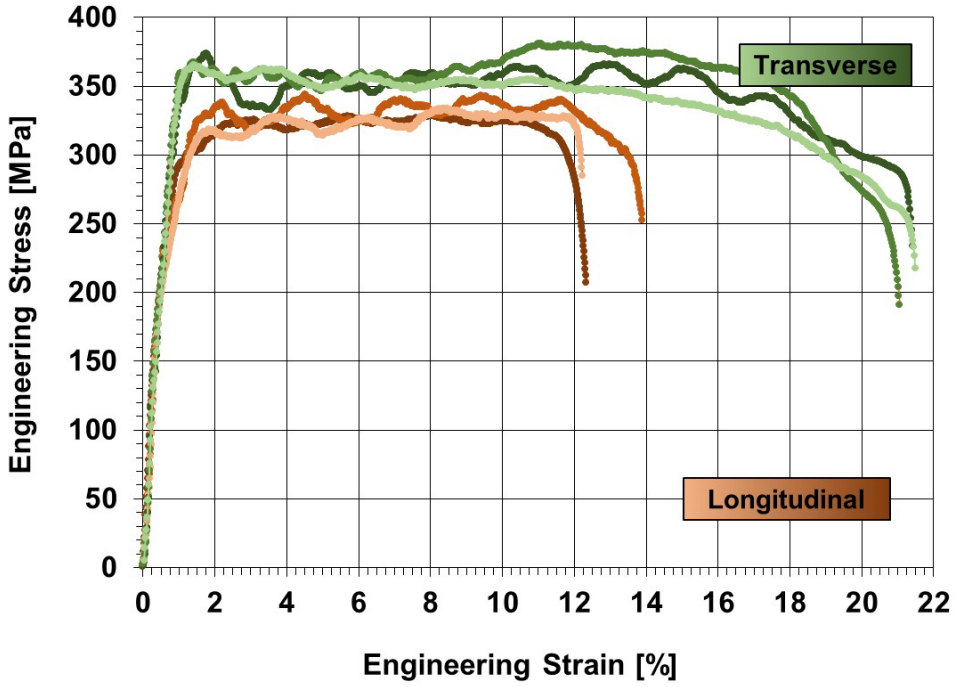

Fig. 26 Engineering stress–engineering strain diagram for samples from the A26 sheet, tested under dynamic tensile loading conditions

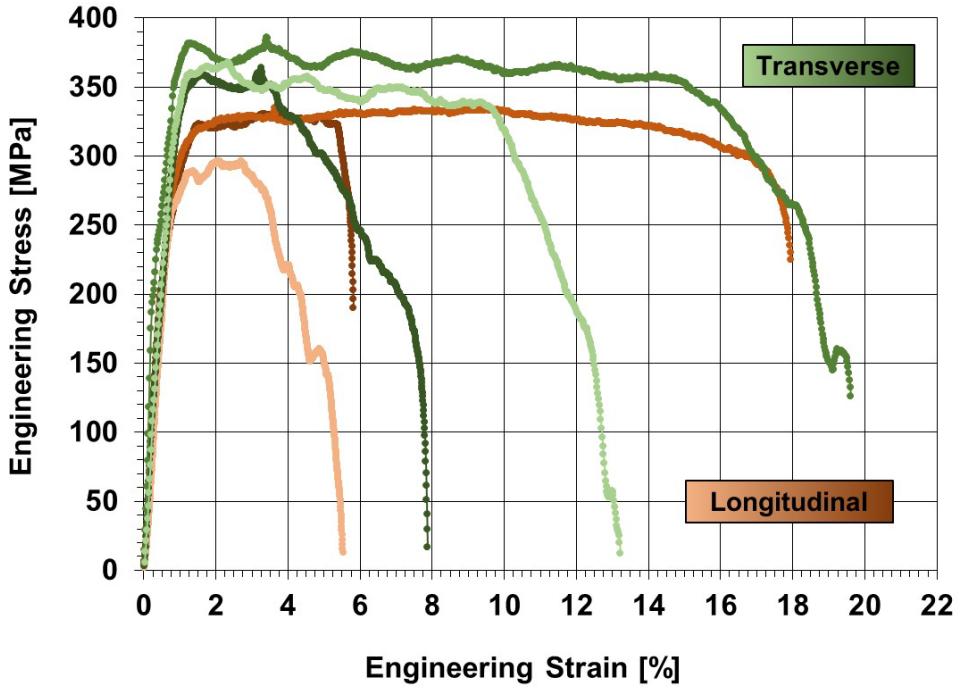

Fig. 27 Engineering stress–engineering strain diagram for samples from the C25 sheet, tested under dynamic tensile loading conditions

Table 5 Mechanical properties of the A26 and C25 sheets under dynamic tensile loading

Specimen	Temperature [°C]	Strain Rate [s^{-1}]	1% Engineering Flow Stress [MPa]	UTS [MPa]	ε_f [%]	q [%]
Dynamic Tensile Tests						
Longitudinal						
A26 Sheet						
A26-long #1	RT	150	305	325	10.7	18.2
A26-long #2	RT	150	325	345	13.2	20.1
A26-long #3	RT	150	310	330	10.7	18.1
Average Value			**313**	**333**	**11.5**	**18.8**
C25 Sheet						
C25-long #1	RT	140	320	330	5.2	7.0
C25-long #2	RT	150	320	330	17.7	16.0
C25-long #3	RT	190	285	290	4.9	6.4
Average Value			**308**	**317**	**9.3**	**9.8**
Transverse						
A26 Sheet						
A26-trans #1	RT	160	350	360	21.5	37.5
A26-trans #2	RT	170	360	380	20.0	33.4
A26-trans #3	RT	160	355	360	21.2	37.4
Average Value			**355**	**367**	**20.9**	**36.1**
C25 Sheet						
C25-trans #1	RT	200	355	360	7.9	8.1
C25-trans #2	RT	160	375	375	18.9	13.1
C25-trans #3	RT	160	360	360	13.1	9.1
Average Value			**363**	**365**	**13.3**	**10.1**

Notes: UTS = ultimate tensile stress; ε_f = elongation to failure; and q = reduction of area (necking to failure); RT = room temperature

3.7 Influence of Strain Rate on the Mechanical Properties of As-Rolled Sheets A26 and C25

Previously, the quasi-static tensile test were performed using specimens with gage lengths of 15 mm and a width of 5 mm ($l_0/b = 3$). Due to the unavailability of sufficient sheet material, the dynamic tests were performed with shorter gage lengths of 9 mm and a width of 3 mm ($l_0/b = 3$). In spite of the different gage lengths and widths, because the aspect ratios were kept the same, the quasi-static and dynamic tensile tests could be compared to one another. Furthermore, the deviations between both specimen geometries were found to be negligible because the material behaved in a brittle manner and an absence of necking was observed.

If the earlier quasi-static results for the A26 and C25 sheets are compared with those obtained in the dynamic tensile tests ($l_0 = 9$ mm, $b = 3$ mm, $l_0/b = 3$), a significant increase in strength with increasing strain rate could be observed. Particularly, as

illustrated by the 1% flow stress and ultimate tensile stress in Figs. 28 and 29, in the longitudinal direction, increases of 10%–20%, and in the transverse direction, increases up to 25%, respectively, were measured at the higher strain rate. Such increases imply that this material in this rolled state is highly strain-rate sensitive.

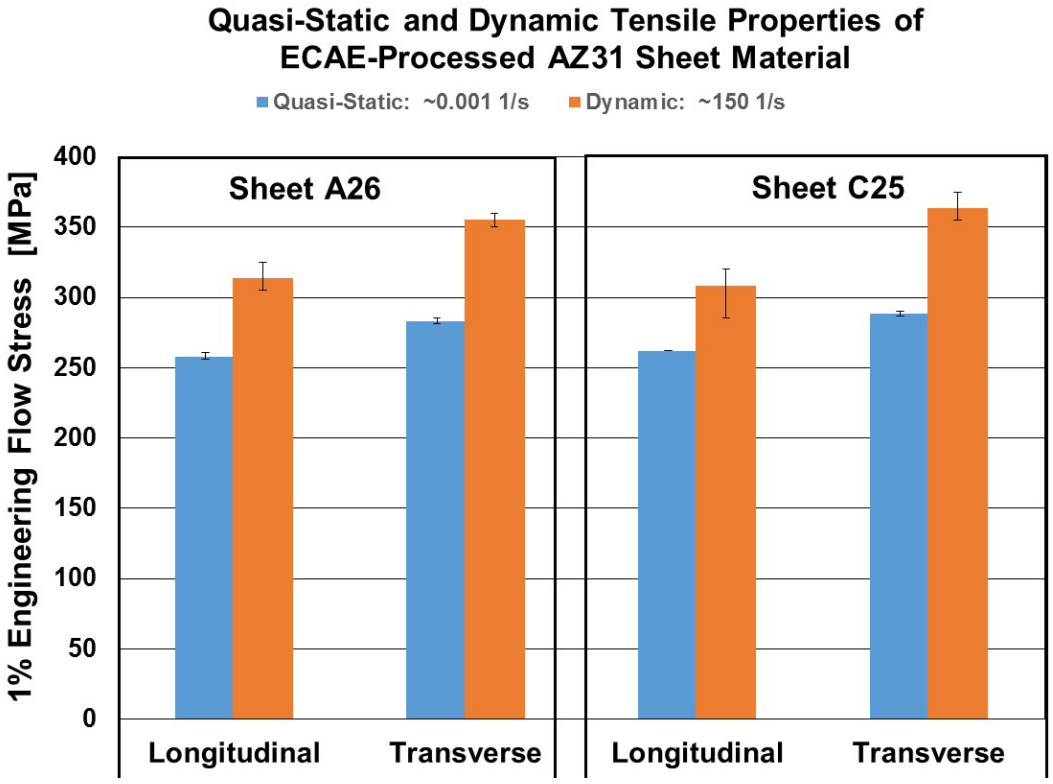

Fig. 28 A comparison of the 1% engineering flow stress obtained from quasi-static and dynamic tensile tests for the A26 and C25 sheets

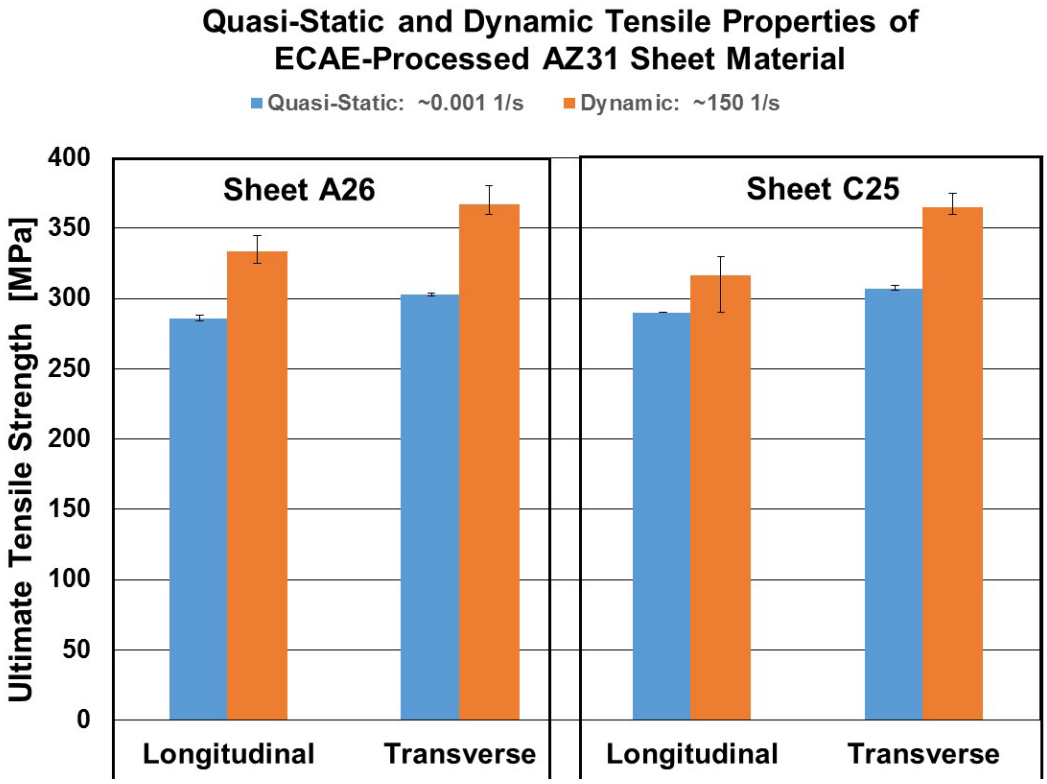

Fig. 29 A comparison of the UTS obtained from quasi-static and dynamic tensile tests for the A26 and C25 sheets

Figure 30 shows the influence of strain rate on the elongation to failure for both sheet types. Interestingly, a roughly constant elongation to failure was determined for sheet A26 with increasing strain rate. However, in contrast, possibly caused by a significant variability in measured ductility values for specimens in both orientations (indicated by the error bars in the histogram, and already noted in the previously displayed stress-strain diagrams, wherein, the spread in the data was quite large), a dramatic decrease in ductility with increasing strain rate can be observed for sheet C25. Because all of the specimen measurements were conducted with good precision and accuracy, it is believed that the most likely reason for this variability could only be explained by defects present (e.g., microcracks) in the as-rolled texture C material. That is, the lower than expected elongation to failure may be introduced during rolling. Specifically, while rolling will tend to realign and even out the highly heterogeneous alternating refined and coarse-grained microstructure of the post-ECAE plate along the rolling and transverse directions resulting in a more uniform strength distribution, it will not homogenize the nonuniform grain size distribution into a more uniform sized grain structure. Therefore, it is quite possible that regions with finer recrystallized grains will remain weaker, causing lower ductility, especially at higher strain rates.

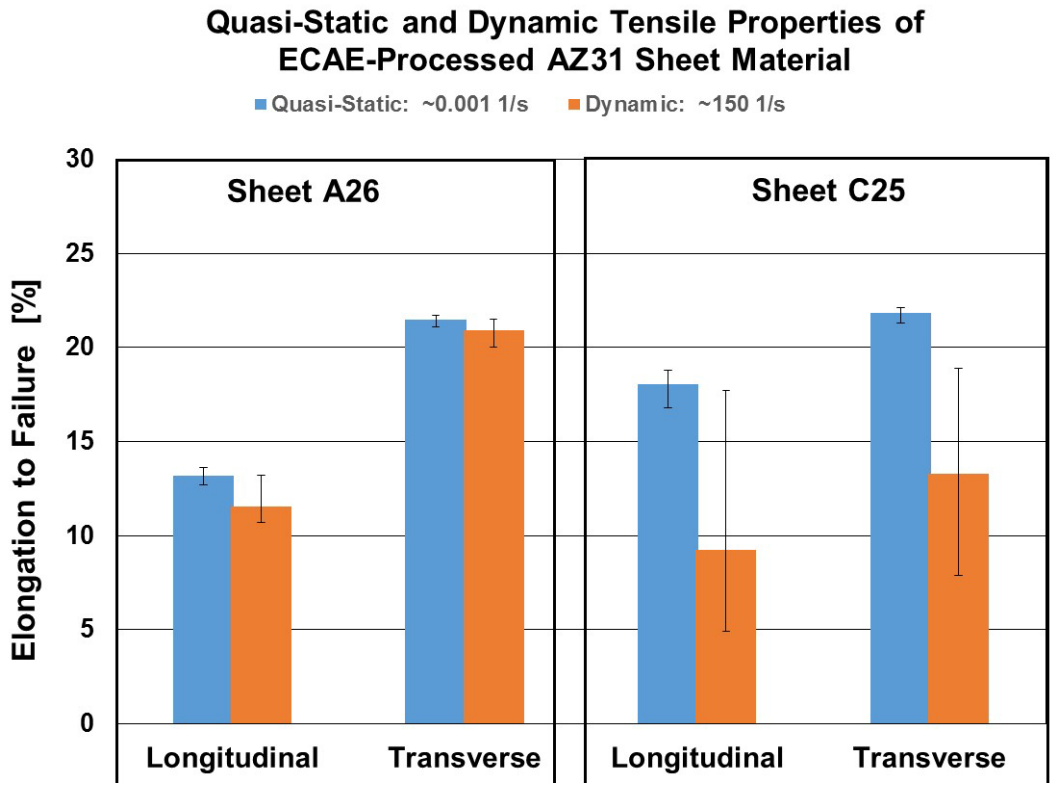

Fig. 30 A comparison of the elongation to failure obtained from quasi-static and dynamic tensile tests for the A26 and C25 sheets

3.8 Fracture Surface Observations of Failed Samples from the As-Failed C25 Sheet

As described in the previous section, significant deviations of the measured elongation to failure of dynamic tensile specimens from the rolled C25 sheet material were observed. In particular, ε_f of 5.2% and 17.7% in samples RSO_C25_long_1 and RSO_C25_long_2, respectively, were measured. Because of this large discrepancy, the fractured failure surfaces were cursorily examined. As expected, different fracture patterns can be observed as shown in Fig. 31. The surface of specimen RSO_C25_long_2 with the larger ε_f fails by smooth shearing with an angle of about 45°. In contrast, the surface of specimen RSO_C25_long_1 is not a smooth sheared surface, but instead, contains a step with a likely brittle cleavage surface coupled with shearing. This may be the result of a different operating failure mode. The study of failure modes was beyond the scope of this study; however, to fully investigate the cause for the apparent difference in failure modes, a more careful SEM analysis of all fracture surfaces in both orientations should be performed.

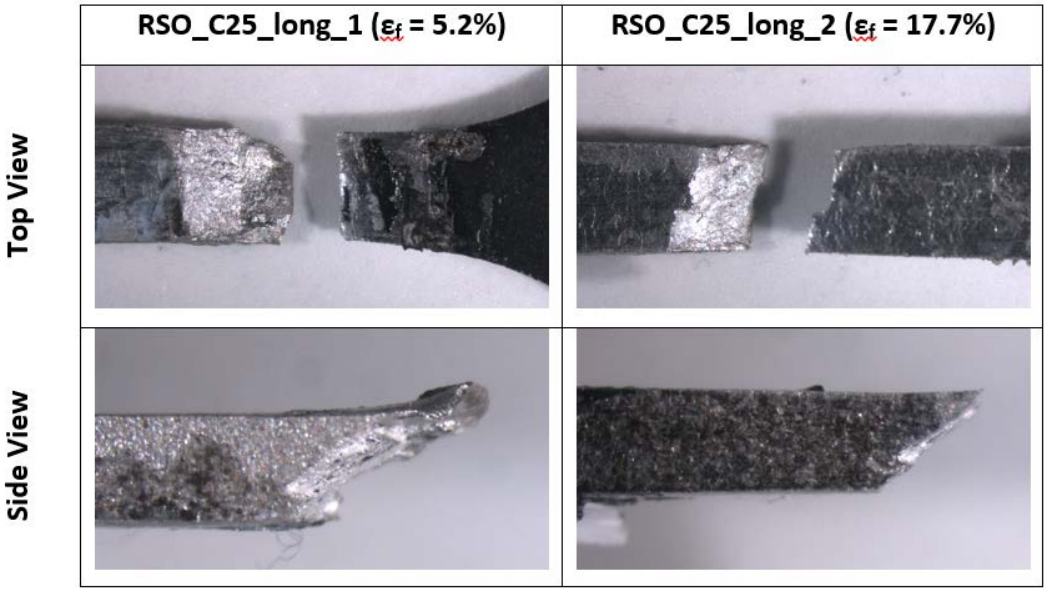

Fig. 31 Fracture patterns of 2 parallel specimens of the C25 sheet. Note the gage width of the specimens is 3 mm.

4. Conclusions

The previously developed rolling schedule for ECAE processed AZ31 Mg alloys, using a rolling temperature of about 275 °C, with a rolling speed of about 1 m/s, and a degree of deformation of about 10% per rolling pass for the first 15 passes and about 20% for the last 3 passes showed very promising results for a second batch of somewhat thicker plates. After 18 passes, the final thickness of the resultant sheet material was about 1.5 mm. Only edge cracks with a length of about 10 to 15 mm could be observed after the final rolling pass. It is likely that the reason for these edge cracks is attributable to inherent defects in the as-received ECAE processed material.

The mechanical properties of the as-received ECAE-processed material were investigated by quasi-static tensile tests at room temperature, and the measured properties were compared with the results obtained for Batch 1.[1] A comparison of the results indicates only slight deviations between these 2 batches. Therefore, if applied consistently, very similar rolling results should be expected.

The as-received ECAE processed plates having texture C were highly heterogeneous, especially in the longitudinal direction. The plates contained zones of uniformly deformed regions, oriented at a roughly 45° slant relative to the extrusion direction. These zones were separated by more heavily deformed zones that appeared like shear bands. However, after rolling, the microstructure was aligned in the rolling direction and consisted of a very fine likely recrystallized

substructure containing some larger grains of about 10 µm. The quasi-static mechanical properties of the plates were consistent with the earlier results for Batch 1, showing higher yield and ultimate strengths in the transverse direction compared to the longitudinal direction. This difference was minimized by rolling the plates into sheet material. Additionally, the sheets possessed better mechanical properties.

Under dynamic tensile loading, at an average strain rate of about 150 s^{-1}, the ECAE processed and rolled sheets for both texture type materials show improved strength levels. For the texture A sheets, the results were more consistent as the elongation to failure was almost constant. However, due to significant deviations in the elongation to failure values for identical specimens from the texture C sheets, a corresponding decrease in ductility with increasing strain rate was observed. Using cursory optical microscopy examination of specimens with different elongations to failure, different fracture surfaces (ductile shear versus a combination of brittle fracture/ductile shear) were observed. The existence of the mixed modes of failure could be a result of microcracks present in the as-rolled material. For a more exact validation of this hypothesis, further SEM analyses should be performed. Regardless, it may be assumed that with a more homogeneous as-received and as-rolled material substructure, better ductility of the texture C sheets could be achieved.

This study only examined the material behavior under uniaxial tensile loading. To fully validate the impact behavior of these Mg sheets in the intended application, multiaxial tension or compression tests are recommended.

5. References

1. Kecskes LJ, Hammond VH, Eichhorst M, Herzig N, Meyer L. Development of rolling schedules for equal channel angular extrusion (ECAE)–processed AZ31 magnesium alloy sheet. Aberdeen Proving Ground (MD): Army Research Laboratory (US); 2016 Apr. Report No.: ARL-TR-7644.

Appendix. Auxiliary Mechanical Property Data for the AZ31 Magnesium (Mg) Alloy Materials

A.1 Part 1: Load–Displacement Curves for the Batch 2 ECAE-Processed Plates

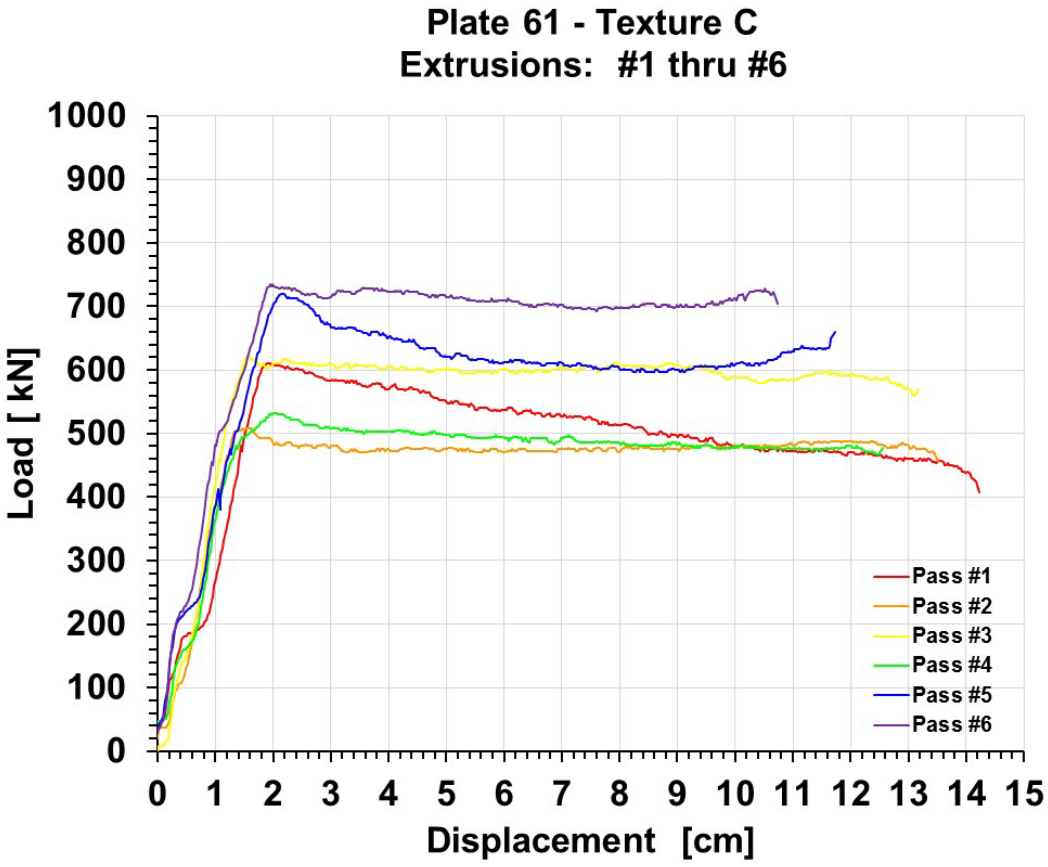

Fig. A-1 Load–displacement curve for equal channel angular extrusion (ECAE) processed Plate 61

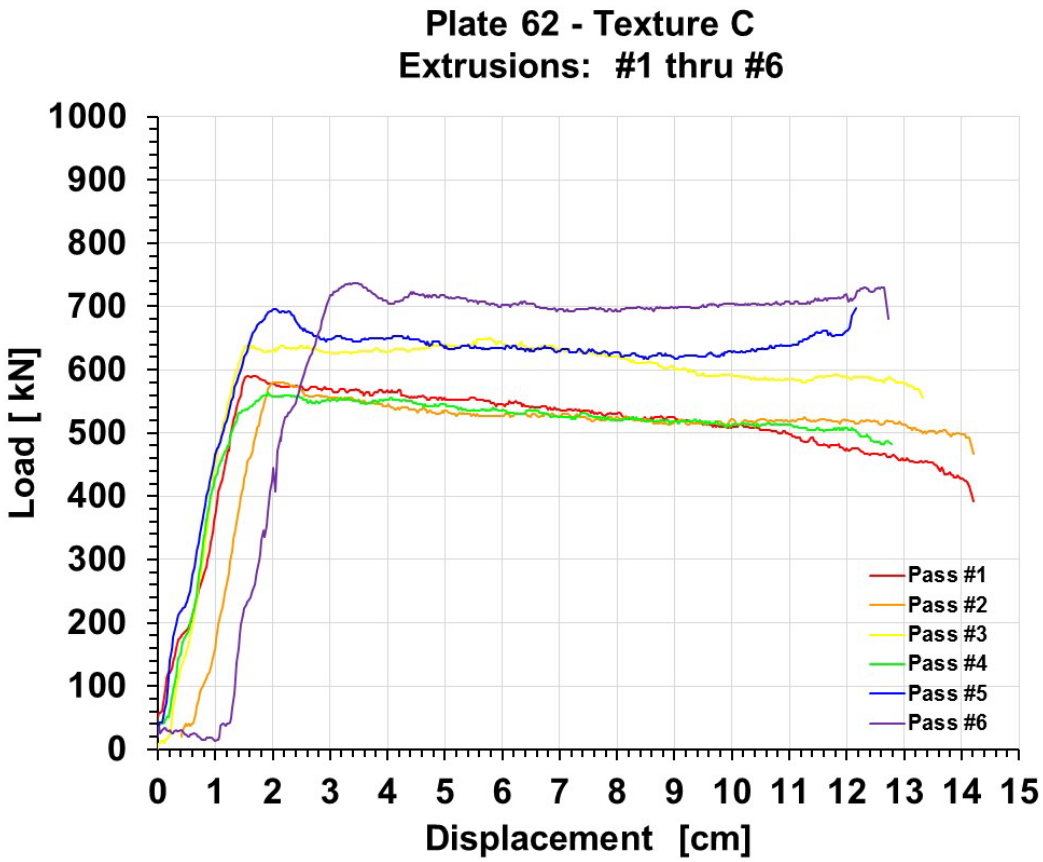

Fig. A-2 Load–displacement curve for ECAE processed Plate 62

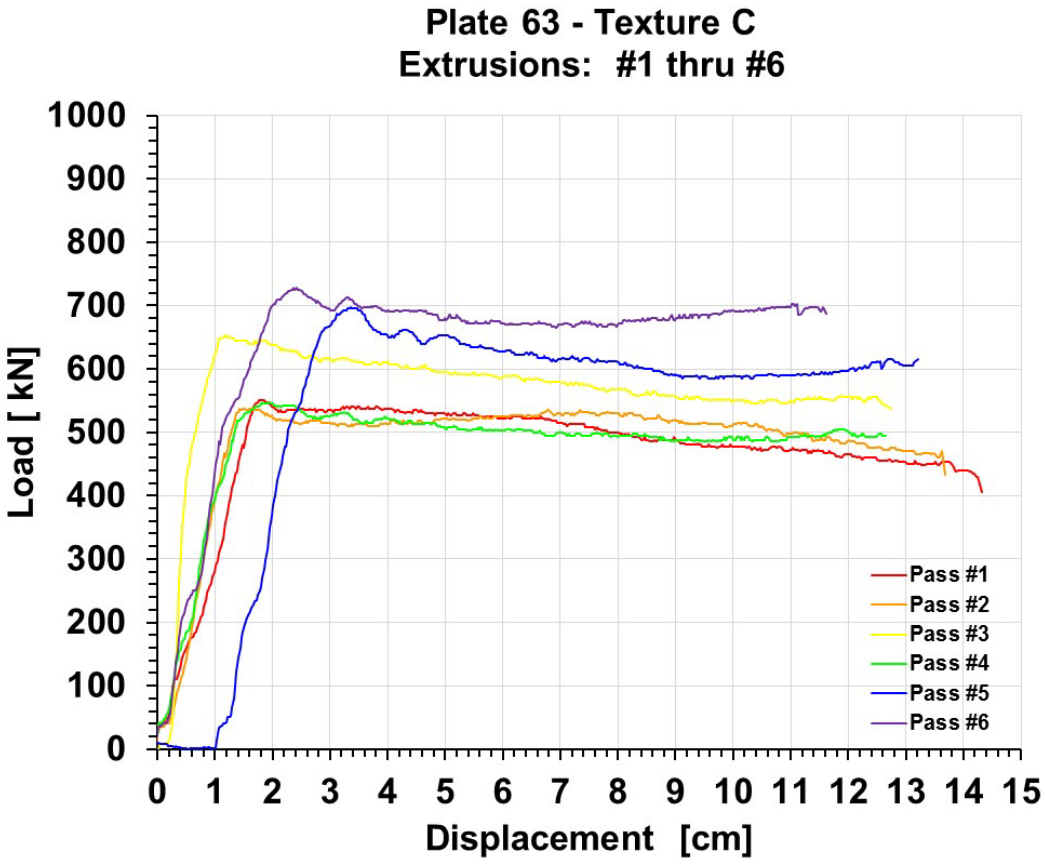

Fig. A-3 Load–displacement curve for ECAE processed Plate 63

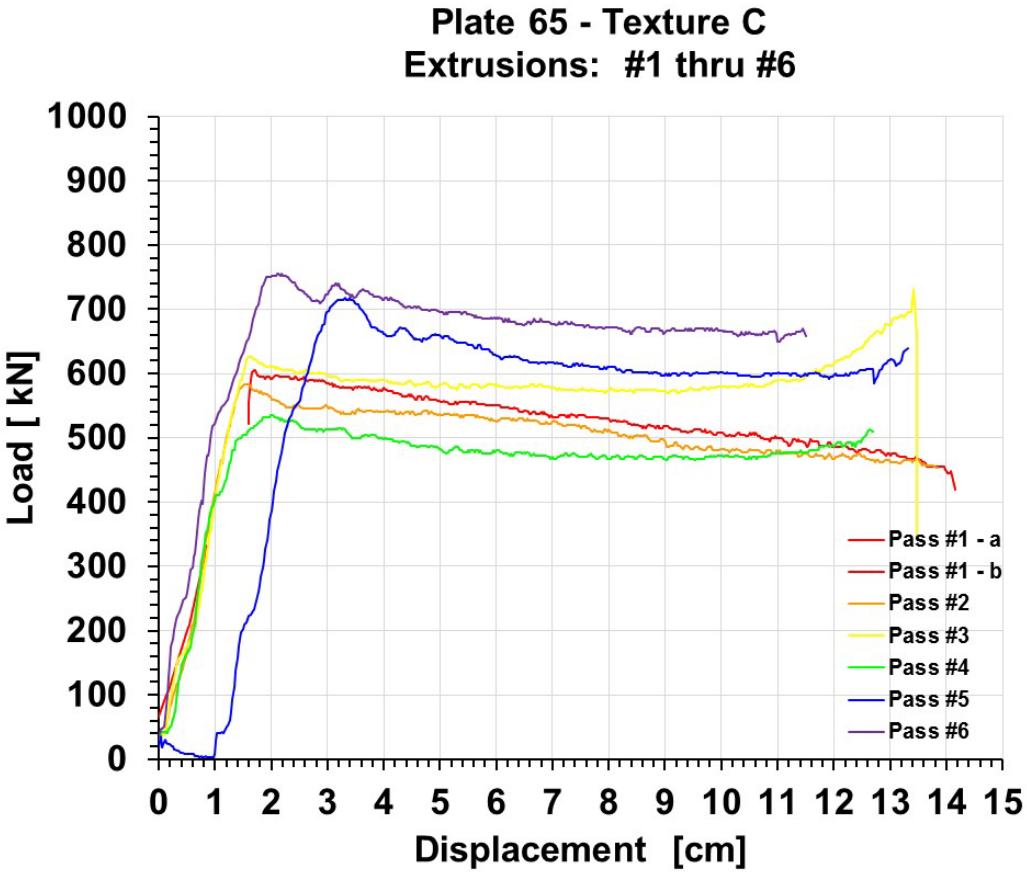

Fig. A-4 Load–displacement curve for ECAE processed Plate 65

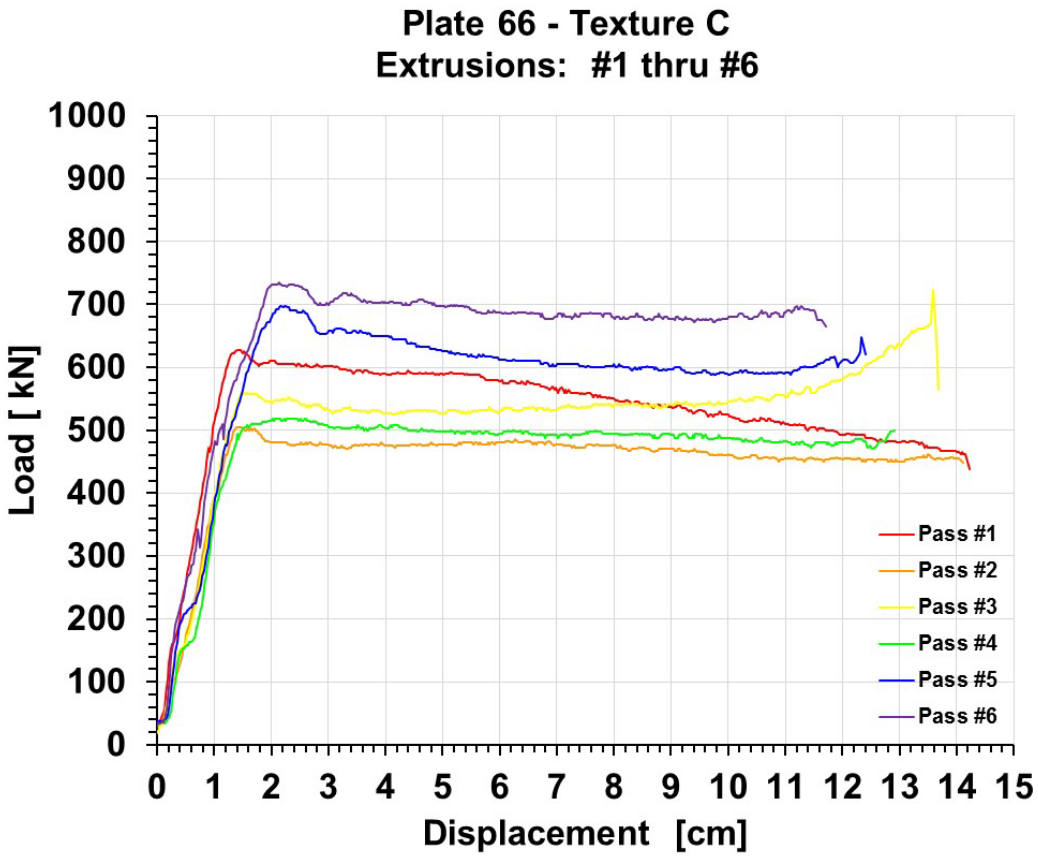

Fig. A-5 Load–displacement curve for ECAE processed Plate 66

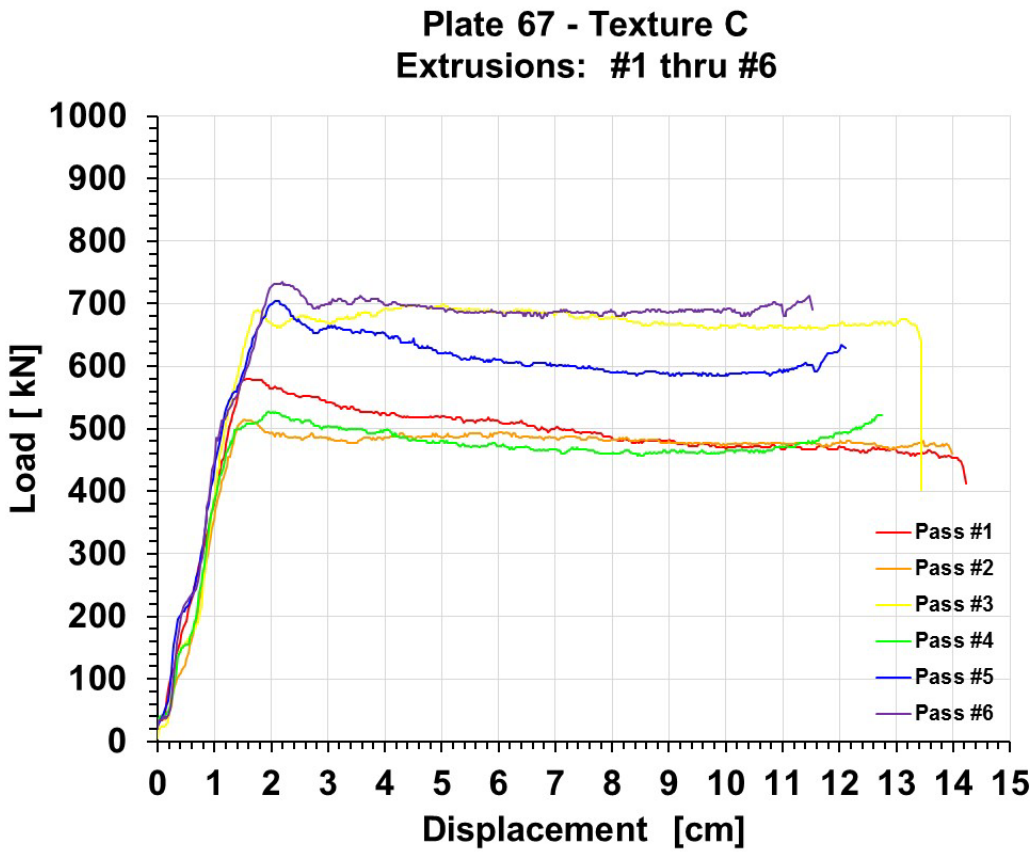

Fig. A-6 Load–displacement curve for ECAE processed Plate 67

A.2 Part 2: Engineering Stress – Engineering Strain Diagrams for the ECAE and non-ECAE AZ31 Mg Plate and Sheet Materials

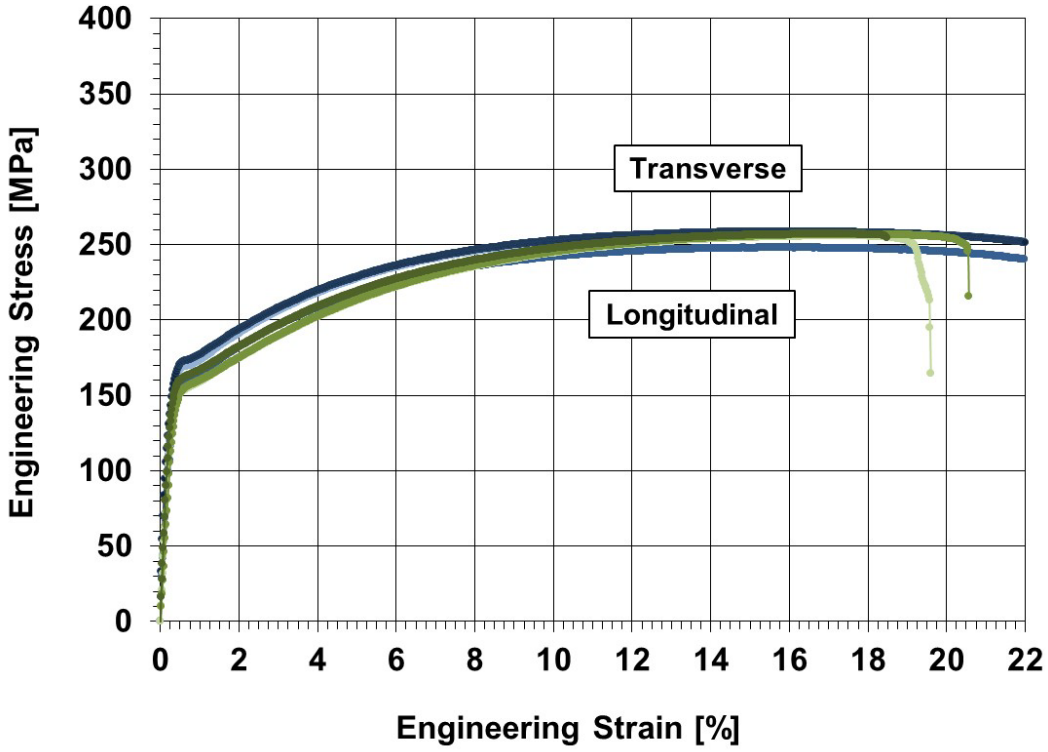

Fig. A-7 Quasi-static engineering stress–engineering strain diagram for Plate 3.1 (as received, no ECAE); 8 rolling passes

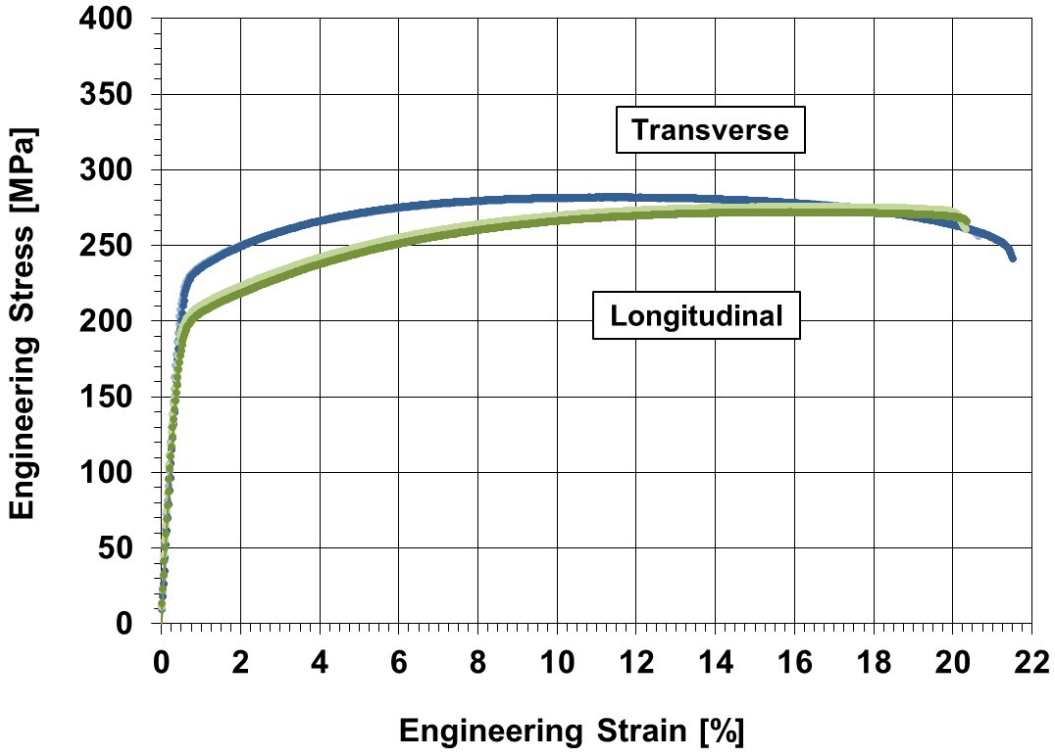

Fig. A-8 Quasi-static engineering stress–engineering strain diagram for Plate 3.2 (as received, no ECAE); 8 rolling passes

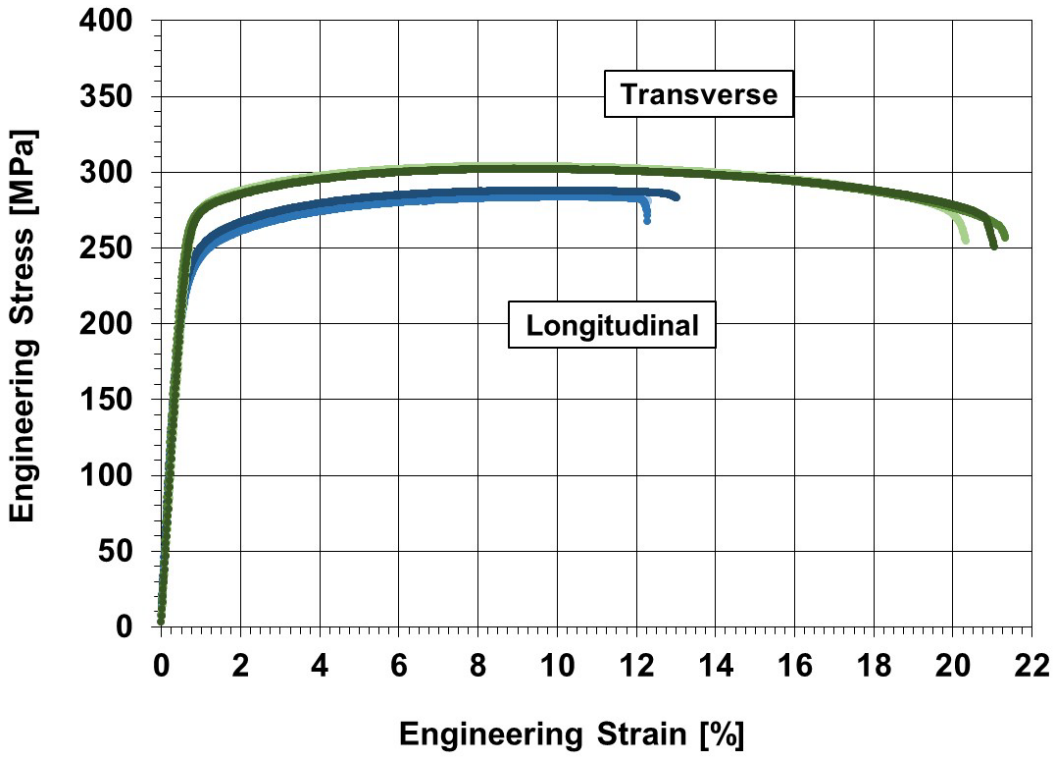

Fig. A-9 Quasi-static engineering stress–engineering strain diagram for ECAE processed Plate 26, rolled into sheet A26; texture A; 14 rolling passes

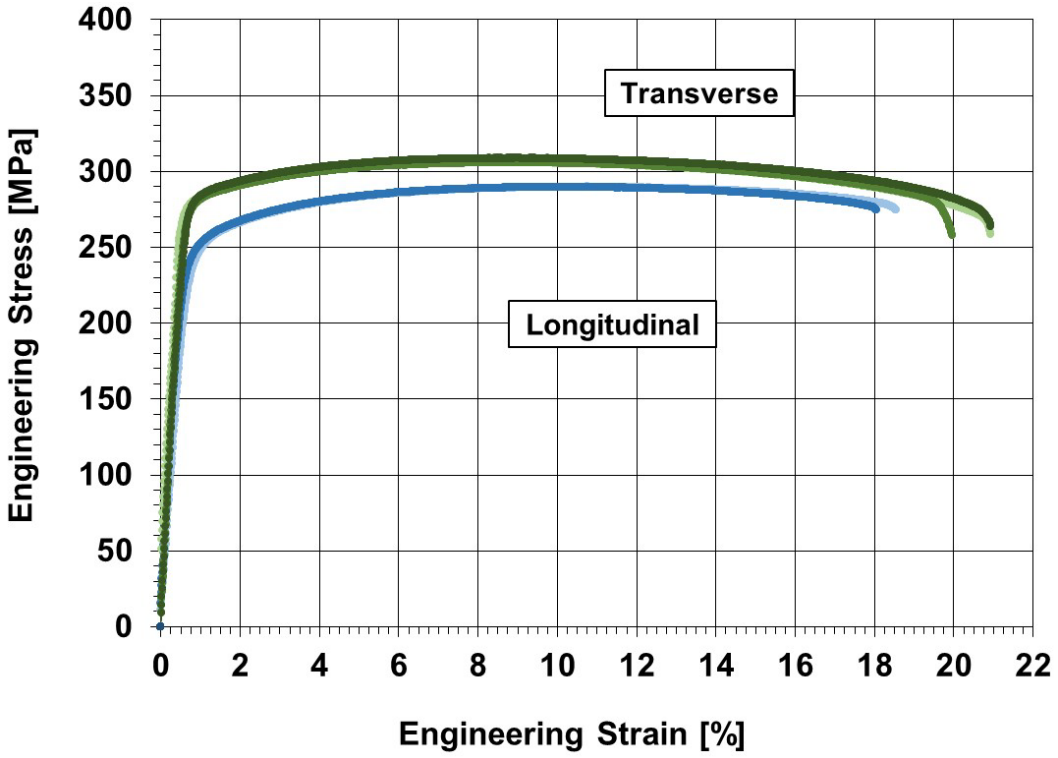

Fig. A-10 Quasi-static engineering stress–engineering strain diagram for the ECAE processed Plate 25, rolled into sheet C25; texture C; 14 rolling passes

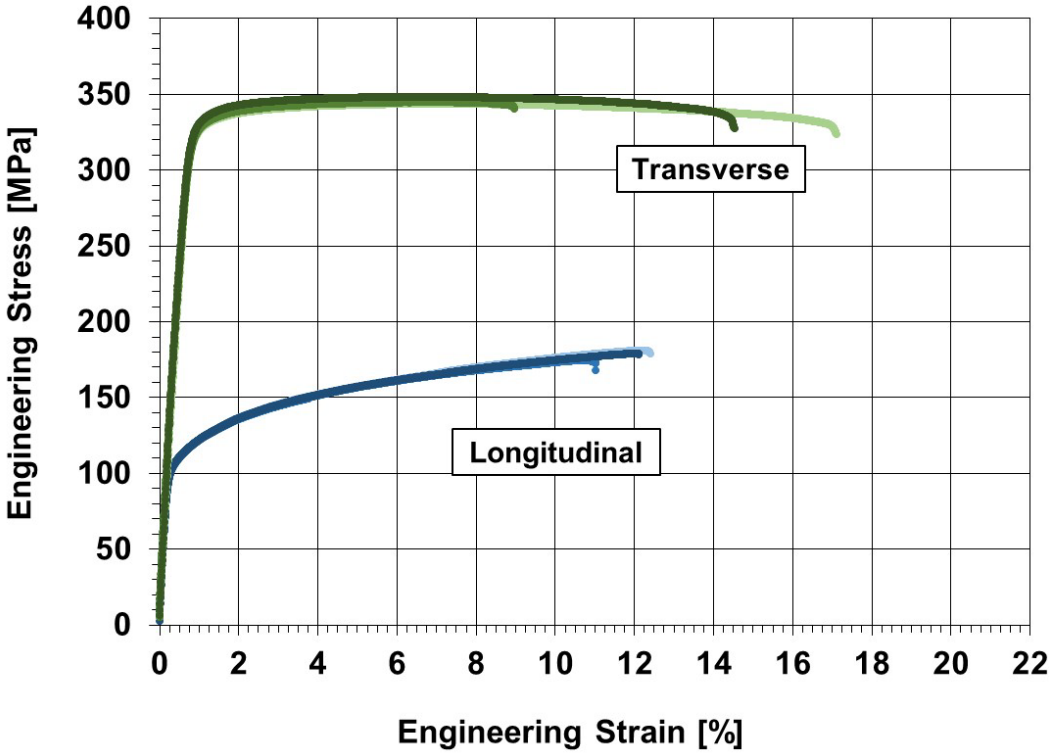

Fig. A-11 Quasi-static engineering stress–engineering strain diagram for ECAE processed plate 13; texture C

List of Symbols, Abbreviations, and Acronyms

ARL	US Army Research Laboratory
ECAE	equal channel angular extrusion
Mg	magnesium
q	reduction of area (necking of failure)
SEM	scanning electron microscopy
UTS	ultimate tensile stress
ε_f	elongation to failure

1 (PDF) DEFENSE TECHNICAL INFORMATION CTR DTIC OCA

2 (PDF) DIRECTOR US ARMY RESEARCH LAB RDRL CIO L IMAL HRA MAIL & RECORDS MGMT

1 (PDF) GOVT PRINTG OFC A MALHOTRA

21 (PDF) DIR USARL
RDRL WMM
J BEATTY
R DOWDING
M VAN LANDINGHAM
RDRL WMM D
R CARTER
K CHO
S WALSH
RDRL WMM E
L VARGAS GONZALES
RDRL WMM F
L DOUGHERTY
S GRENDAHL
V HAMMOND
E HORWATH
L KECSKES
T SANO
M TSCHOPP
RDRL WMP C
R BECKER
D CASEM
J LLOYD
C WILLIAMS
RDRL WMP E
M BURKINS
T JONES
P SWOBODA